José Nilton Tavares Barbosa

Lic. em Engenharia Mecatrónica

PV Inverters for Module Level Applications

Dissertação para obtenção do Grau de Mestre em
Energias Renováveis – Conversão Eléctrica e Utilização Sustentáveis

Orientador: Doutor João Martins, Professor Auxiliar, FCT-UNL

Co-orientador: Doutor Luis Pina, Coordenador de I&D, WS Energia

FACULDADE DE CIÊNCIAS E TECNOLOGIA
UNIVERSIDADE NOVA DE LISBOA

Setembro 2011

Dedicated To My Dear Family

You Are My Inspiration

Acknowledgements

First, and foremost, I must thank my family for the unconditional support in every aspect of my life, and in particular for the enormous effort to provide me a good education, despite all the difficulties. I would like to thank also, every one that for one way or another gave his contribution for my personal, social or academic training responsible for each success I have. I thank my tutor and co-tutor, Dr. João Martins and Dr. Luis Pina respectively, for all the support during the development of this project. I thank the WS Energia S.A for the opportunity to cooperate and learn with them. Finally and not less important I thank my friends and colleagues for all the help and support, especially those that always believed in me, and have been I real fellows in this journey. "*Without friends no one would choose to live, despite having all other goods.*" - *Aristotle*

Abstract

Nowadays, the photovoltaic (PV) energy is presented as one of the most promising source of clean energy, and so a good way for greenhouse gas emissions mitigation and reduce the fossil fuel dependence. Within it, the photovoltaic energy has caused a huge interest in the electronic converters, and the need to improve their efficiency and reducing their cost. With this work I present a solution for a module scale grid-connected single-phase inverter. The solution consists in a two-stage inverter insolated with a grid line transformer. The two-stage inverter is composed by a DC-DC converter and a DC-AC converter connected through a DC-link capacitor. The DC-DC converter in case is a boost converter used to elevate the voltage from the PV module to a higher level. For the DC-AC converter it is used a full-bridge inverter, and both the DC-DC and the DC-AC converters use the IGBTs form an integrated module with its respective drivers. To the boost control it is implemented a Maximum Power Point Tracking algorithm that can optimize the power extraction from the PV source and for the inverter it is used a sliding mode hysteretic control. Once this inverter is conceived to work connected to the grid, a single-phase PLL system is used to synchronize the injected current to grid voltage. All the control part is made digitally using an Arduino Uno board, which uses an Atmel microcontroller.

Keywords: Inverters, Microinverters, Photovoltaic, Power Electronics, Renewable Energies.

Resumo

Atualmente, a energia fotovoltaica é apresentada como sendo uma das mais promissoras fontes de energia limpa, e assim uma boa maneira de mitigação das emissões dos gases com efeito de estufa e reduzir a dependência dos combustíveis fósseis. Com ele, a energia fotovoltáica tem despertado um enorme interesse nos conversores electrónicos, e na necessidade de melhorar a sua eficiência e reduzir os seus custos. No presente trabalho apresenta-se uma solução para inversores monofásicos ligados à rede à escala de modulos. A solução consiste em um inversor de dois estágios com transformador de isolamento. O inversor de dois estágios é composto por um conversor DC-DC e outro DC-AC conectados atravez de um condensador de barramento DC. O conversor DC-DC no caso é um conversor boost utilizado para elevar a tensão do modulo fotovoltáico para um nível superior. Para o conversor DC-AC é utilizado um inversor de ponte completa e para ambos os conversores são utilizados IGBTs de um módulo integrado com seus respectivos drivers. Para o controlo do boost é implementado um algoritmo de rastreamento do ponto de máxima potência que optimiza a extração de energia da fonte PV e para o inversor é usado o controlo de modo de deslizamento das correntes. Uma vez que este inversor é concebido para funcionar conectado à rede, é usado um sistema de PLL monofásico para sincronizar a corrente injectada com a tensão da rede. Todo o controlo é feito digitalmente usando uma placa Arduino Uno que usa um microprocessador da Atmel.

Palavras-cháves: *Inversores, Microinversores, Electrónica de Potência, Fotovoltáico, Energias Renováveis.*

Table of Contents

List of Figures

List of Tables

List of Abbreviations

AC – Alternated Current

BJT – Bipolar Junction Transistor

Bps – bits per second

DC – Direct Current

EPIA – European Photovoltaic Industry Association

HF – High Frequency

IGBT – Insolated Gate Bipolar Transistor

LF – Low Frequency

MOSFET – Metal Oxide Semiconductor Field Effect Transistor

MPP – Maximum Power Point

MPPT – Maximum Power Point Tracking

NPT – Non Punch-Through

NTC – Normal Temperature Conditions

PI – Proportional-Integral

PLL – Phase Loop Lock

PT – Punch-Through

PV – Photovoltaic

PWM – Pulse Width Modulation

THD – Total Harmonic Distortion

VCE – Collector-Emitter Voltage

Chapter 1

Introduction

1.1 Scope - PV Inverters

PV systems transform the solar energy from light into Direct Current (DC), usually low voltage, while most electric devices use 230V or 110V Alternated Current (AC). PV inverters are the devices used to convert the energy delivered from the photovoltaic arrays from DC mode to AC in order to be injected to the grid network or to be consumed by the majority of the electric devices and machines.

1.2 Motivation

The inverters are studied and used for a while in the Power Electronics. They are not a new concept. There are many technologies and electronic devices that can be used to build them. But with the recent interest in the photovoltaic energy employment, the interest in this kind of electronic converter largely increased. As any energy converter, there are always losses in the way and the efficiency could never achieve 100%. So, many studies were done to reduce these losses and improve the efficiency. Nowadays, we have inverters with almost 99% of efficiency under certain conditions. So this could lead us to think that there is not much to improve because the inverter technology is mature with high efficiency.

The inverters used today in the PV power plant, or domestic plant are essentially the central inverters or the string inverters. In the central inverters, all the panels are jointed in a single inverter which does the electronic work. The string inverter plant uses an inverter for each line of panels. The generation of energy by a PV plant is made individually module by module or more precisely cell by cell. So when the MPPT is done for a group of panels it represents the maximum power point for the whole group which does not correspond to the maximum power point of each individual module or cell. This mismatching results in losses, even more significant than those that come from the electric conversion. One way to mitigate this problem is to distribute the electronic converters for each PV module and so each one work on the module

MPP. The inconvenient of this solution is that it is now needed to replace the single central inverter with several module level inverters, rising cost and maintenance issues.

1.3 Objective

The mainline objective of this work is to develop a practical, reliable and cost-effective solution for a module scale inverter that could be connected directly into the grid network. This is the first step of the WS Energia's strategy to enter the PV inverter's market so, the following three main objectives arise:

1) Study all technologies suitable for module level PV inverters.
2) Select one of these technologies and produce a prototype.
3) Provide a clear technical outlook for the next steps of WS Energia's strategy.

To achieve these, simulations of the various topologies in the desired scale must be made using the MatLab-Simulink software, their outcomes must be analyzed, so that the selected solutions can be implemented and experimented on. At the end, an experimental prototype controlled digitally and ready to be tested in the field must be available.

1.4 Contributions

This work is the first step that will guide WS Energia through its strategy to commercialize high-efficiency inverters on the PV market. The contributions can be summarized as follows:

1) Selection of the most promising inverter architectures.

   Several possible architectures were proposed, simulated and compared so that an informed choice can be made.

2) Prototype of the most promising architecture.

   A module level inverter prototype was produced and tested to further study the selected architecture and to explore the practical implementation difficulties.

3) Provide knowledge and information to arrive at a successful product.

   The acquired knowledge clarified all technical issues related to the conception of a module level inverter.

1.5 Thesis organization

This thesis is organized in six chapters. The first chapter provides an introduction for the whole work including a short overview about PV inverters, the motivation to make this research and development, the objectives that I propose to be accomplished and the contribution that this thesis is for the science and technology, and how it is organized. The second chapter refers to the stat-of-the-art of the PV inverters technology including their types and topologies. In chapter three I describe the simulation of the various topologies and presented their results. In the fourth chapter it is simulated the chosen topology including its control and the various parts that it is built in a more precise manner. Chapter five describes in detail the project implementation such as the materials and the hardware used, and presents the results of the experimental tests. At the sixth and last chapter it is exposed the conclusions and the future continuation of this work.

Chapter 2

Photovoltaic Inverter Technology – State of the Art

2.1 General issues on photovoltaic energy

Photovoltaic technology uses sunlight to generate electricity. Sunlight is a renewable energy source that could theoretically be exploited to supply energy abundantly for an infinite time into the future. Completely free of cost, sunlight is widely available on Earth regardless of geographical location. On the other hand, the intermittency of sunlight causes the operation of PV to rely directly on the time of day and weather. On a cloudy day or at night, the power supply is diminished or cut off unless some other source of electricity is used. Additionally, the power density of sunlight is low (1 kW/m^2 in clear conditions), so large-scale PV electricity production requires either a large area covered with PV modules or mirrors for concentrating sunlight on a smaller area.

The power generated by a PV module depends on the module technology and on the intensity of sunlight. The power that a module produces at a given moment is proportional to the perpendicular sunlight intensity on the module surface. Power is therefore reduced if conditions are cloudy or if the angle of incidence of sunlight is large. In general, the average power production of a PV system can be reliably estimated on a monthly basis from previously measured meteorological data. Shorter time intervals introduce uncertainty, but weather forecasts can well be used to predict power production one day in advance.

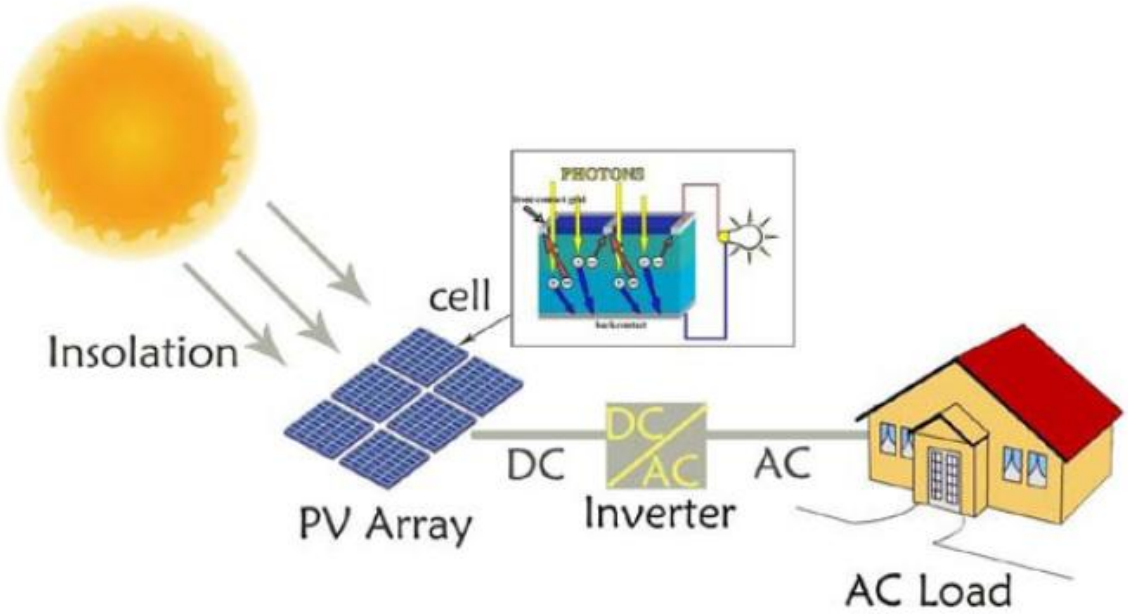

Fig. 2.1: Photovoltaic Energy System

From: Duffy And Cathcart, 2008

PV arrays can be built ranging from a few watts up to several megawatts due to their modular design. Existing arrays can always be expanded to meet growing electricity demand, although the electronics in the system may need updating.

Nowadays, the major drawback of photovoltaic electricity is its high price. When a lot of power is needed, PV system is seldom cost-effective. However, in small-scale consumption such as in residential buildings, the competitiveness of PV electricity is improving. While the initial investment into a PV system demands capital, operation and maintenance require next to nothing. (Ross and Royer, 1999)

2.1.1 Environmental and Economical Motivations

Photovoltaic technology provides clean energy: sunlight acts as the fuel and there are no harmful emissions or polluting gases released during operation. In particular, PV systems do not produce any CO2 emissions when operating, so they can be used to cut greenhouse gas emissions. Apart from operation, PV systems nevertheless carry the environmental weight of other stages in their life cycle. (Alsema and Nieuwlaar, 1997; EPIA and Greenpeace, 2004; Battisti and Corrado, 2005)

One of the main environmental concerns with photovoltaic modules is the hazardous substances involved in the production of the modules, including large volumes of acid and alkaline etchants as well as smaller amounts of toxic lead (EPIA, 2004). In addition, certain PV technologies have specific needs: for example, some thin-film technologies require cadmium and selenium for production. However, the hazardous substances used in PV technology are deposited in a very stable and fixed way in the solar cell and therefore pose hardly any threat to the environment (Ross and Royer, 1999). The risks concerning the toxic materials used in photovoltaics should not be exaggerated as long as their disposal is properly attended to. (Alsema *et al*, 1997; Fthenakis, 2004)

Photovoltaic systems can also be evaluated in terms of energy pay-back time. Energy payback time illustrates the time taken for power generation to compensate for the energy used in production. For photovoltaic modules it is typically 2 to 4 years, which amounts to approximately 10% of their expected lifetime (EPIA and Greenpeace, 2004). The payback time decreases when system become more efficient, so considerable reductions up to less than one year or 3% is anticipated in the future (PV-TRAC, 2005).

In improving the cost-effectiveness of photovoltaic systems, most of their environmental impacts are bound to go down as well: the impacts are mainly associated with material use or processes that will have to be eliminated or optimized. Since new advances are constantly reported, the performance and cost limits have evidently not been met, and there are still plenty of improvements to be performed before optimal production is reached. (Ross and Royer, 1999; Sørensen, 2000) As the environmental impact of the module production decreases, the role of the other components will become more important in terms of the energy efficiency of the whole PV system (Alsema and Nieuwlaar, 1997).

2.1.2 The Need for Efficient Electronic Converters

As said above, the sunlight energy is abundant in all Earth (1 kW/m^{2}of overall power density), but the known technology of today can only take profit of part of it. Photovoltaic cells are the most developed technology to convert directly the sun energy into a usable energy like electricity. However, the efficiency of conversion is still low compared with other technologies (4 to 30%). The higher performance PV cells are under development nowadays, especially using different sunrays concentration techniques. As is well known, electronic converters are essential for the PV systems once there is the necessity to convert electric quantities into those that match

with most electric devices or public grid for instance. So, for the all system effectiveness, as in cost, reliability and performance, it is not only necessary good cells. Optimal electronics devices are indeed required.

2.2 PV Inverters

An inverter, or DC-AC converter, is an electrical device that converts direct current (DC) to alternating current (AC); the converted AC can be at any required voltage and frequency with the use of appropriate transformers, switching, and control circuits. Photovoltaic cells are DC power suppliers, so it is necessary the use of an inverter to feed the AC devices or to connect the PV system to the grid.

According to the plant topology we have many different types of PV inverters, such as central inverters for wide power range from 1 kW to up to 100 kW or even more, string inverters and module inverters. Central inverters are used in large applications. Many times they can be connected according to the "master-slave" criteria, when the succeeding inverter switches on only when enough solar radiation is available or in case of main inverter malfunction. Inverters connected to module strings are used in wide power range applications allowing for more reliable operation. Module inverters are used in small photovoltaic systems.

2.2.1 Central Inverters

This kind of inverters is essentially used in the larges PV power plants, where several strings are connected in parallel.

Characteristics:

- Three fase
- Power range: 10 kW – 250 kW
- High electric efficiency
- Low cost/kWp
- Low reliability
- MPPT at the installation level

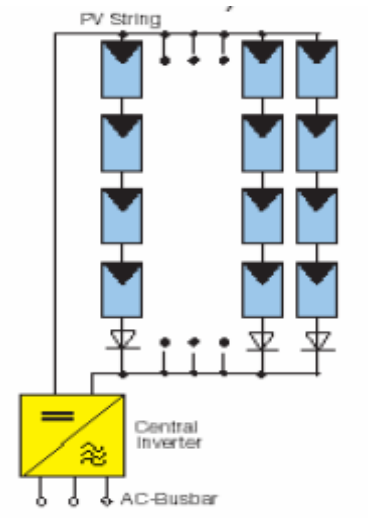

Fig. 2.2: Central inverter

2.2.2 String Inverters

In this kind of configuration there is one inverter for each string, and is typically used in middle scale application.

Characteristics:

- Power range: 1.5 kW – 5 kW
- MPPT a string level
- Different string orientation possibility
- Three-phase inverters for power > 5 kW

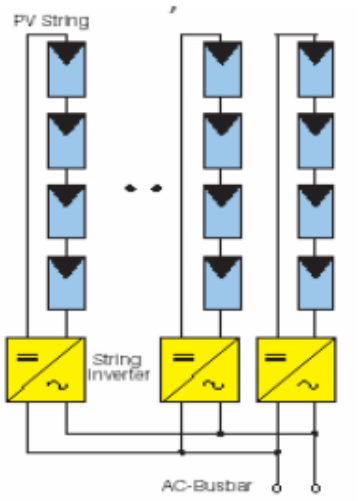

Fig. 2.3: String Inverters

2.2.3 Module Inverters

In this configuration each panel has its own inverter.

Characteristics:

- Power range: 50 – 300 W
- MPPT at module level
- Low efficiency
- Difficult maintenance
- High cost/kWp

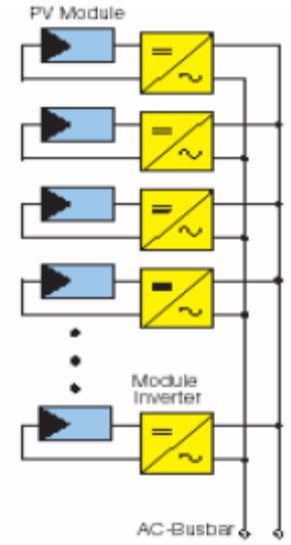

Fig. 2.4: Module inverters

Note: the images from fig. 2.2, 2.3, 2.4 is imported from http://www.volker-quaschning.de

2.3 PV Inverters Topologies

In order to achieve better results on the energy conversion, some components can be added to the system. Components as a DC/DC converter, a power transformer and filters are usually used. The usage or not of these different components gave birth to the existence of many inverter topologies for PV systems.

These topologies are essentially classified by the number a flour, the number of voltage levels, and the kind of isolation.

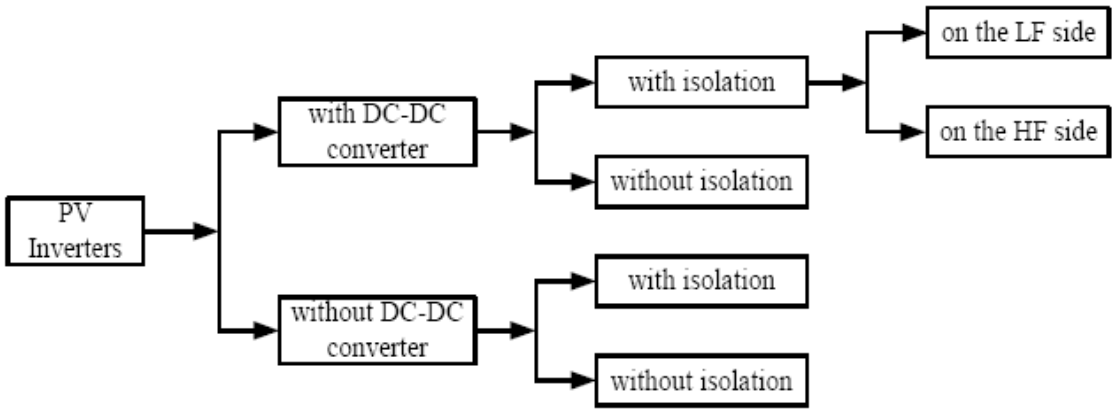

Fig. 2.5: Tree of Inverters topology
from: Liserre et al, 2004

2.3.1 PV inverter with DC/DC converter and galvanic isolation

This topology is widely used in the PV systems, especially for residential applications connected to the grid. The DC/DC converter is used to operate the PV arrays at the maximum power point (using MPPT algorithm). The transformer is used to elevate the voltage to a value similar to the grid. It also provides protection against external current discharge.

2.3.1.1 Using transformer on low frequency (LF) side

In this topology type, the transformer is connected between the DC/AC converter and the grid, as shown in the fig. 2.6.

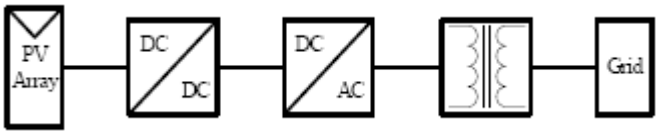

Fig. 2.6: PV inverter with DC/DC converter and galvanic isolation sing transformer on low frequency (LF) side - diagram

In this case, the transformer is operating in the same frequency as the DC/AC converter output and the grid. It provides a good isolation to the PV inverter system.

2.3.1.2 Using transformer on high frequency (HF) side

In this topology the transformer is located into the DC/DC converter box leading to a more compact solution (fig. 2.7). However, it increases the design complexity.

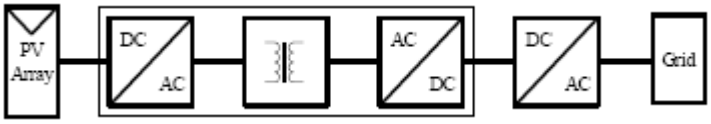

Fig. 2.7: PV inverter with DC/DC converter and galvanic isolation using transformer on high frequency (HF) side - diagram

In fig. 2.8, we have a typical solution with push-pull DC/DC converter with HF transformer and PWM full-bridge inverter with filter.

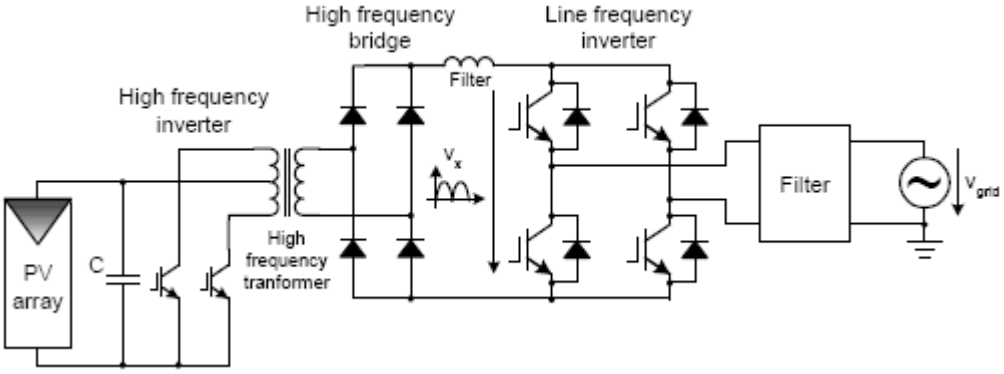

Fig. 2.8: PV inverter with DC/DC converter and galvanic isolation using transformer on high frequency (HF) side

2.3.2 PV inverter with DC/DC converter

This is a typical transformerless system, where we have a boost converter to elevate the output voltage. It has a compact design, and it is very competitive in cost and simplicity.

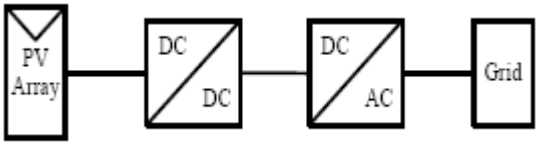

Fig. 2.9: PV inverter with DC/DC converter – diagram

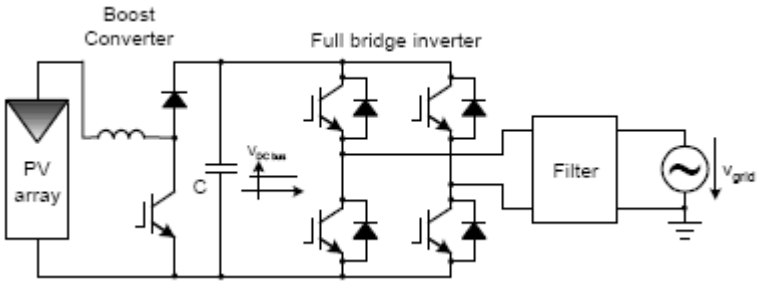

Fig. 2.10: PV inverter with boost

This converter system can achieve efficiency higher than 96% (Blaabjerg, 2006).

2.3.3 PV inverter without DC/DC converter with galvanic isolation

This is a simple topology where the inverter receives the energy directly from the PV array. Normally a capacitor is used between these components in order to have an uncoupling of energy and stabilization of the output voltage. To elevate the voltage till a value comparable with the grid, power transformer is used on the AC side of the inverter.

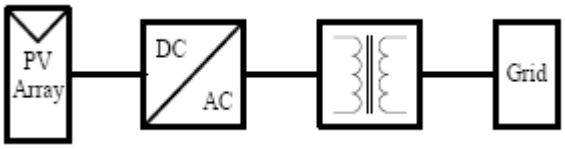

Fig. 2.11: PV inverter without DC/DC converter with galvanic isolation – diagram

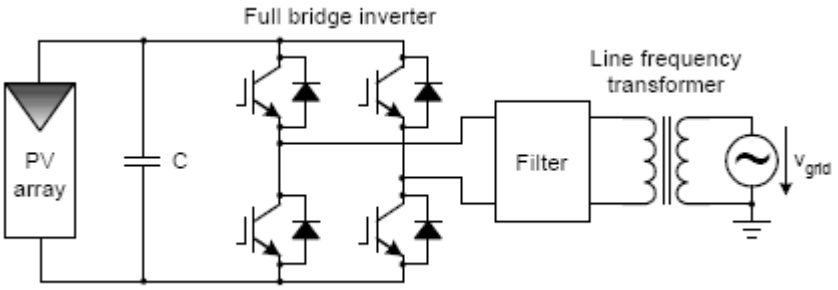

Fig. 2.12: PV inverter without DC/DC converter with galvanic isolation

2.3.4 PV inverter without DC/DC converter and isolation

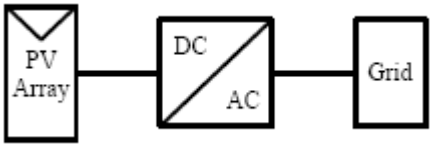

Fig. 2.13: PV inverter without boost and galvanic isolation - diagram

This is the simplest scheme for a PV inverter system. Once there is no boost converter or power transformer to elevate de voltage, it requests high level of input DC voltage.

Solution with full-bridge inverter

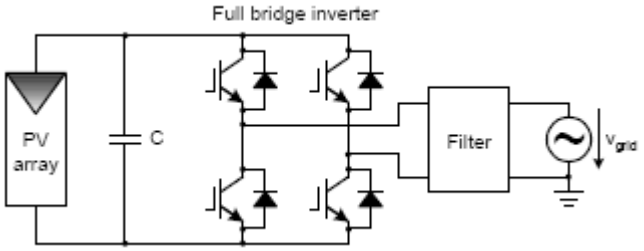

Fig. 2.14: PV inverter without boost and galvanic isolation - Solution with full-bridge inverter

Multi-level solution for low dc input

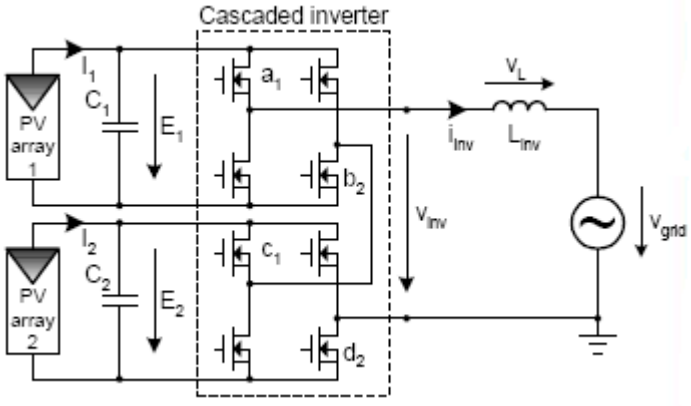

Fig. 2.15: PV inverter without boost and galvanic isolation - Multi-level solution for low DC input

2.4 Pulse Modulation Schemes

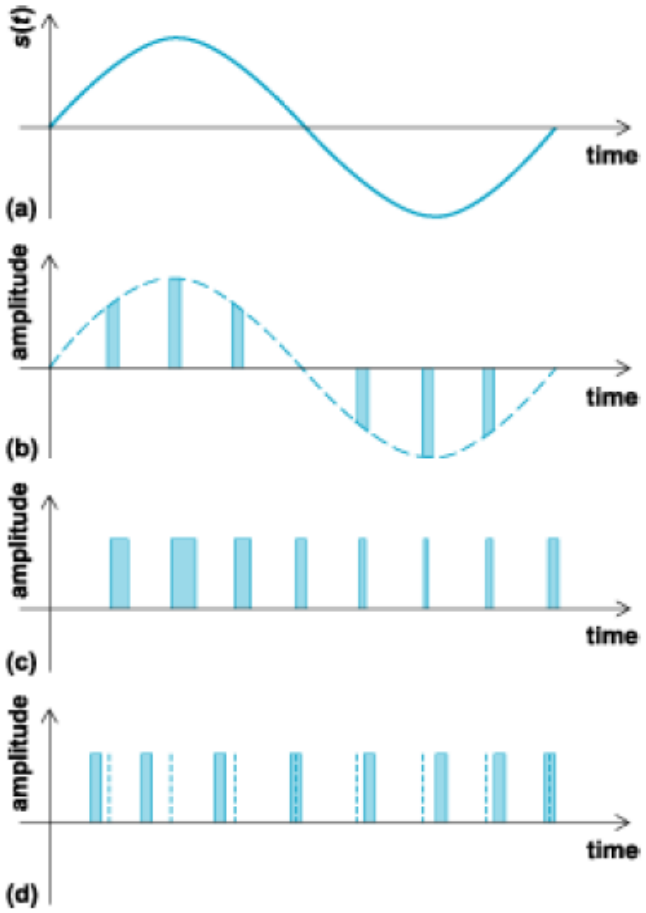

Fig. 2.16: (a) Analog signal s(t). (b) Pulse amplitude modulation. (c) Pulse width modulation, (d) Pulse position modulation
From: Mohanty and Sahoo, 2010

The signal modulation technique defines the quality of output signal. The quality measure for a sine wave signal is THD (Total Harmonic Distortion).

Advantages of Pulse-Width Modulation (PWM)

- ✓ The output voltage control is easier with PWM than other schemes and can be achieved without any additional components.
- ✓ The lower order harmonics are either minimized or eliminated altogether.
- ✓ The filtering requirements are minimized as lower order harmonics are eliminated and higher order harmonics are filtered easily.
- ✓ It has very low power consumption.
- ✓ The entire control circuit can be digitized which reduces the susceptibility of the circuit to interference.

2.4.1 Two levels modulation

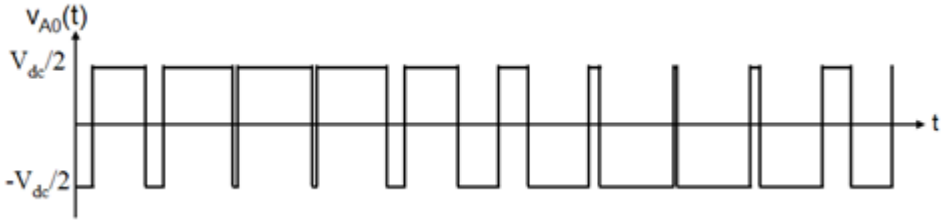

Fig. 2.17: Two levels modulation

The fig. 2.17 represents the output signal of a two level inverter. This king of inverter is largely used due to its simplicity in the circuits and control. It requires also few numbers of switches witch make it very easy to be built.

2.4.2 Multi-level modulation

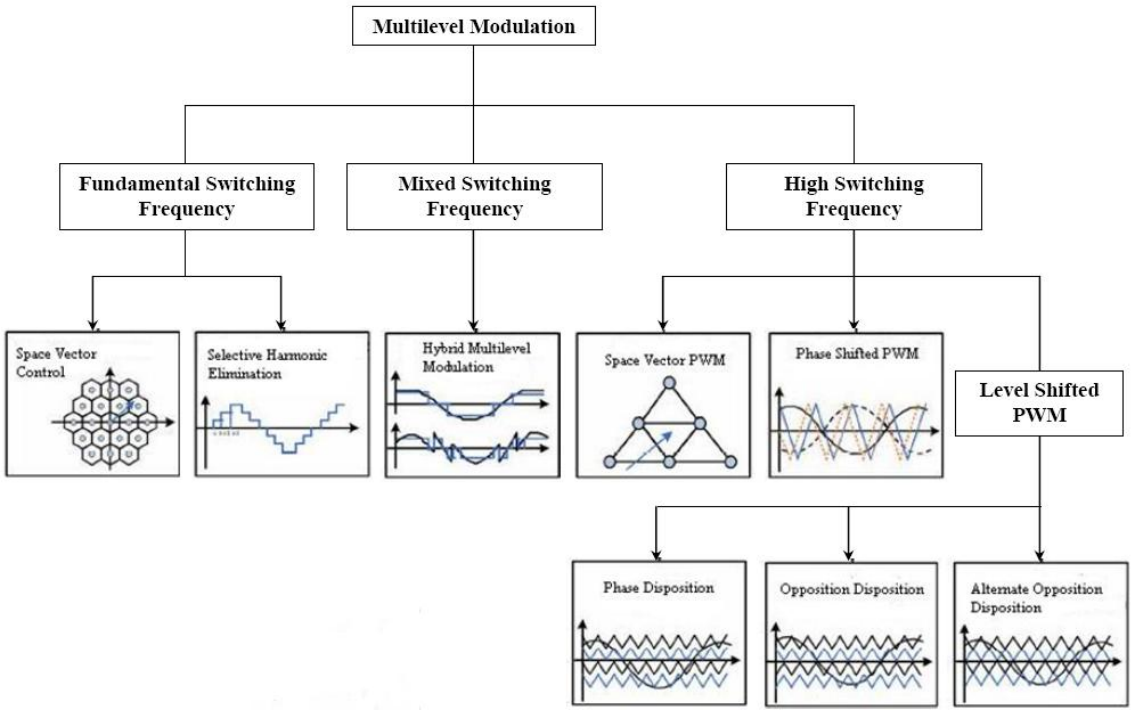

Fig. 2.18: Multilevel modulation scheme
From: LEGA, 2007

The fig. 2.18 shows the many variation of Multilevel Modulation as Fundamental Switching Frequency, Mixed Switching Frequency, High Switching Frequency and Level Shifted PWM. The

Fundamental Switching frequency is often used once it requires low switching frequency and presents good quality of the output signal. The quality of the signal is as better as much is the number of voltage levels as shows the fig. 2.19, 2.20 and 2.21.

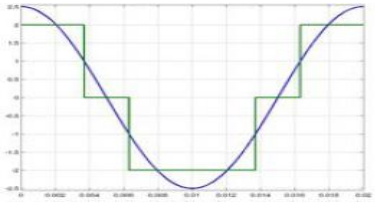

Fig. 2.19: Three levels inverters signal

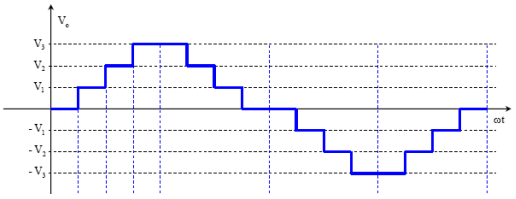

Fig. 2.20: Seven levels inverters signal

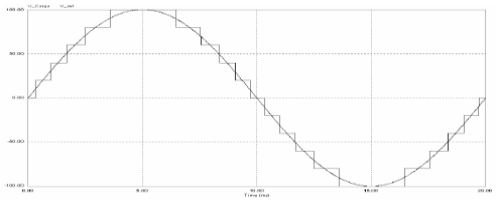

Fig. 2.21: 11 levels inverter signal

2.5 Harmonic Distortion

Harmonic distortion is the change in the waveform of the supply voltage from the sinusoidal waveform. It is caused by the interaction of distorting customer loads with the impedance of the supply network. The ideal low voltage single phase supply is 230 Vrms, at a frequency of 50 Hz and with a sinusoidal waveform as shown in Fig. 2.22.

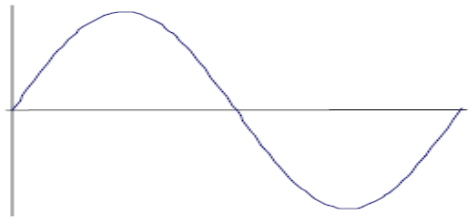

Fig. 2.22: Ideal sinewave

Until the 1960s, most customer loads drew a current waveform which was also sinusoidal. Such loads include induction motors, incandescent lights, stoves and most household appliances. The actual power system voltage can depart from the ideal sinewave in several aspects. When every cycle of the wave form is distorted equally the deficiency is called harmonic distortion.

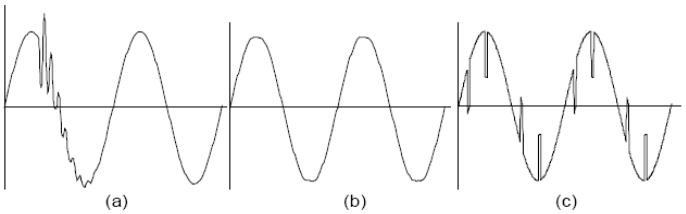

Fig. 2.23: Types of voltage distortion: (a) Non-harmonic distortion, (b) flat-top harmonic distortion, (c) notching harmonic distortion.
From: GOSBELL *et al*, 2000

2.6 Energy Storage in Grid-connected PV Plants

In grid-connected PV plants, theoretically, energy storage is not necessary or useful, due to the availability of the distribution grid that should work as an ideal container of the electrical energy (theoretically, it can work both as an ideal generator and, also, as an ideal load). However, in these last years, an important attention has been devoted to the use of energy storage also in grid-connected PV plants, with the main aim of overcoming some important power quality problems of real distribution grids and for making PV plants more and more useful and attractive (Carbone, 2010).

There are many types and technologies for energy storage like batteries, super-capacitors, super-magnetics, flywheels, pumped-hydro, compressed air, hydrogen… and their main outcome is that energy storage systems are on the basis of the achievement of very important and valuable ancillary services, able to significantly improve reliability, availability and power quality of modern distribution grids.

Advantages of energy storage in electricity distribution grids**:**

- The energy storage adds value to distributed generation plants from renewable by making them predictable;
- Satisfying the peaks of the load demand;
- compensate for load variations, so making possible to operate transmission, sub-transmission, and distribution networks with lighter designs;
- Energy storage facilitates the active and reactive power flow control for distribution grid voltage regulation;
- Energy storage at power plants may provide "black-start" capability (power for plants that need electricity to start up);
- Energy storage may have special use in applications such as momentary carry-over for short outages to high-value industrial processes and/or plants, voltage support, power factor correction and other aspects of power quality;
- Energy storage facilitates the interconnection among different generation plants from renewable (solar, wind, fuel-cells...) and may make them more reliable and efficient;
- Taking advantage of the new contest of the free market of the electrical energy, in a distribution grid with energy storage systems, electrical energy can be purchased during a low load demand, at low rates, can be stored and, then, can be sold, during a peak of the load demand, at a higher rate.

2.6.1 Batteries in Grid-connected PV Systems

The use of batteries in grid-connected PV systems is largely applied by many reasons as those said above, and also, because of the losses that can be avoided with its presence.

2.6.2 Losses caused by the mismatching between the PV plant and the grid

These losses occur when the power injection capability of the PV plant mismatches the power absorption capability of the grid. By considering the grid fully passive and resistive, for the sake of simplicity, this problem can be appreciated with the help of (a), in which the working point of

the system composed by the PV plant and the grid is graphically found by superimposing the I-V characteristic of the PV plant with the I-V characteristic of the grid.

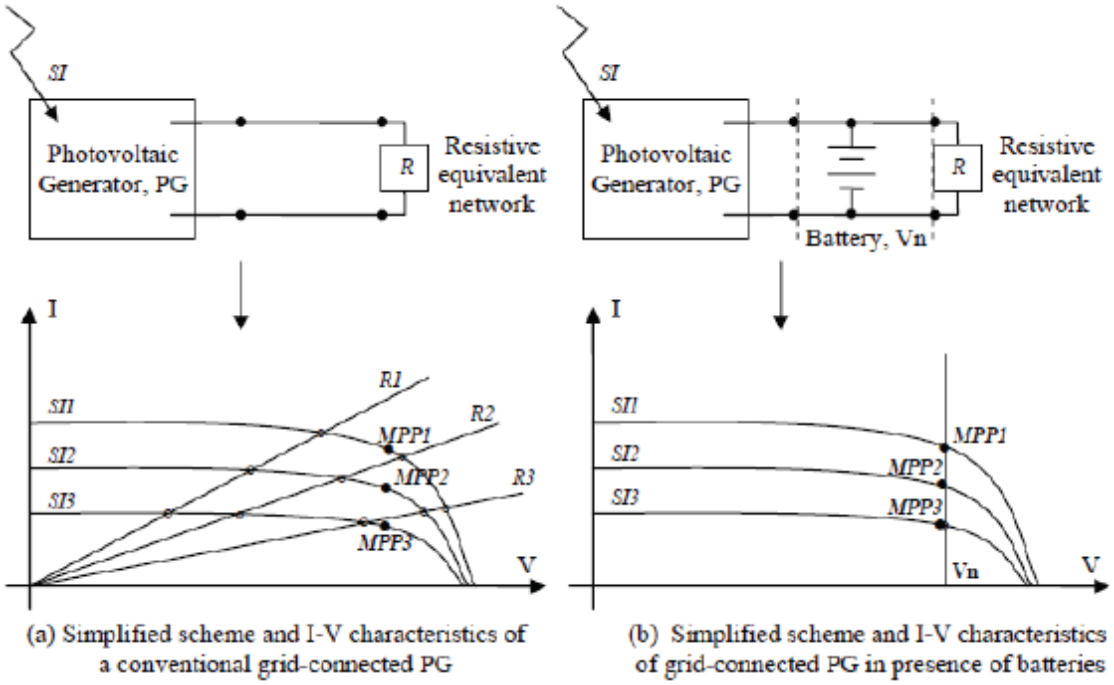

Fig. 2.24: Batteries in grid-connected PV systems
From: CARBONE, 2010

2.6.3 Losses caused by mismatching conditions among PV modules of the PV plant

The mismatching in working conditions of different PV modules of the same PV plant can occur, essentially because of:

- Discrepancies in module parameter values caused by manufacturing tolerances;
- different module ageing effects;
- Different orientations of modules.

Furthermore, especially in a urban residence, where PV modules of a PV plant are normally installed on the rooftops, shadows created by clouds, neighbor buildings, trees, power and telephone lines, sometimes partially cover PV modules (partial shadowing), and creating a condition of mismatching or “unbalanced generation” among different PV modules.
In case of mismatching conditions, the current generated by a PV string is physically imposed to be equal to the minimum current value, corresponding to the current generated by the most unfavorably irradiated PV module of the PV string, and, finally, the whole power generated by

the PV string can be reduced with respect to the maximum available power. In order to alleviate the aforementioned problem, traditionally, a bypass diode is connected in parallel with each PV module; this alleviates the power reduction of the PV string, however, the shaded PV modules cannot generate their inherent power, and hence the problem has now its optimal solution.

2.6.4 Losses caused by the reversed power flow on grids

Radial power distribution grids are designed for a power flow from the high voltage (HV) side to the low voltage (LV) side. In presence of Grid-connected PV plants, power flow is reversed from the end of LV side to the HV side of grids and this may cause voltage rise of LV line. To prevent the over voltage of the power distribution lines, power electronic inverters for PV plants have a function that regulate the output power when the voltage of the grid is too high; because of this function, significant amount of electric power of PV plants can be lost [Ueda et al., 2006].

2.6 MPPT techniques

One of the most diffused techniques used to optimize the energy production on PV plants is known by Maximum Power Point Tracking (MPPT). MPPT is a control technique that presents an optimal electrical load to solar panel or array and produces a voltage suitable for the load.

2.7.1 Active MPPTs

Active MPPTs are based on algorithms precisely conceived to maximize the power injected into the grid by a PV plant. Using this technique you can avoid the Losses caused by the mismatching between the PV plant and the grid, described above. These algorithms can be directly implemented on single-stage (DC-AC) PWM inverters; however, usually they are more profitably implemented on double-stage (DC-DC and DC-AC) PWM inverters, in which the DC-DC power electronic converter (widely, a boost type converter) is specifically devoted to the implementation of the selected MPPT algorithm. There are lots of different MPPT algorithms, characterized by different performances.

2.7.2 Batteries as passive MPPTs

Batteries, connected in parallel with a PV field, can operate as a passive MPPT, without use of any additional circuit or implementation of the control logic. A battery in parallel with a PV system and the grid, when its properly designed in its nominal voltage value and its capacity, it

can naturally, catch a maintain the working point of the PV system very close to the MPP for any solar irradiation level and for any value of the network equivalent resistance.

As it is expected, batteries used as passive MPPT has lower performance if compared with currently utilized active MPPTs, mainly because of the variation of the PV voltage caused by the variation of working temperature. Because of this consideration, as an alternative to the trivial idea of utilizing batteries in grid-connected PV systems in a centralized way and in the place of active MPPTs, it is proposed to use batteries in large grid-connected PV plants and in a more effective “distributed way” (Carbone,2010).

2.7 Switching devices Technology

2.8.1 MOSFET

Metal Oxide Semiconductor Field Effect Transistor (MOSFET) is based on the original field-effect transistor introduced in the 70s. The invention of the power MOSFET was partly driven by the limitations of bipolar power junction transistors (BJTs) which, until recently, were the devices of choice in power electronics applications.

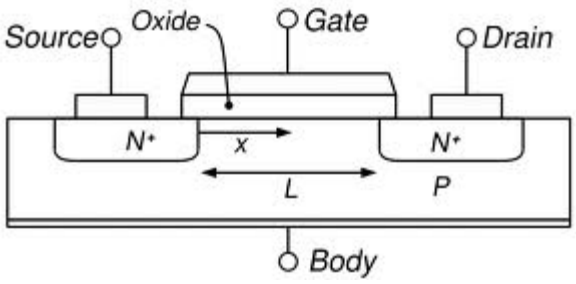

Fig. 2.25: MOSFET

2.8.2 IGBT

Combining an easily driven MOS gate and low conduction loss, Insolated Gate Bipolar Transistor (IGBT) quickly replaced power bipolar transistors as the device of choice for high current and high voltage applications. The balance in tradeoffs between switching speed, conduction loss, and ruggedness is now being ever finely tuned so that IGBTs are encroaching upon the high frequency, high efficiency domain of power MOSFETs. In fact, he industry trend is for IGBTs to replace power MOSFETs except in very low current applications.

To determine which IGBT is appropriate for a particular application, the following parameters must be taken in count:

Operating voltage - the highest voltage the IGBT has to block should be no more than 80% of the collector-emitter voltage (VCE) rating;

Hard or soft switched – a PT device is better suited for soft switching due to reduced tail current, however a NPT device will also work (The PT and NPT concepts are explained in the next sub-section);

The current that will flow through the device – For hard switching applications, the usable frequency versus current graph is helpful in determining whether a device will fit the application;

The desired switching speed - If the answer is “the higher, the better”, then a PT device is the best choice. Again, the usable frequency versus current graph can help answer this question for hard switching applications.

Short-circuit withstand capability – for applications such as motor drives, the answer is yes, and the switching frequency also tends to be relatively low.

The operation of an IGBT is very similar to a power MOSFET. A positive voltage applied from the emitter to the gate terminals causes electrons to be drawn toward the gate terminal in the body region. If the gate-emitter voltage is at or above the threshold voltage, electrons are drawn toward the gate to form a conductive channel across the body region, allowing current to flow from the collector to the emitter. Therefore, an N-channel IGBT is basically an N-channel power MOSFET constructed on a p-type substrate, as illustrated by the generic IGBT cross section in Fig. 2.26.

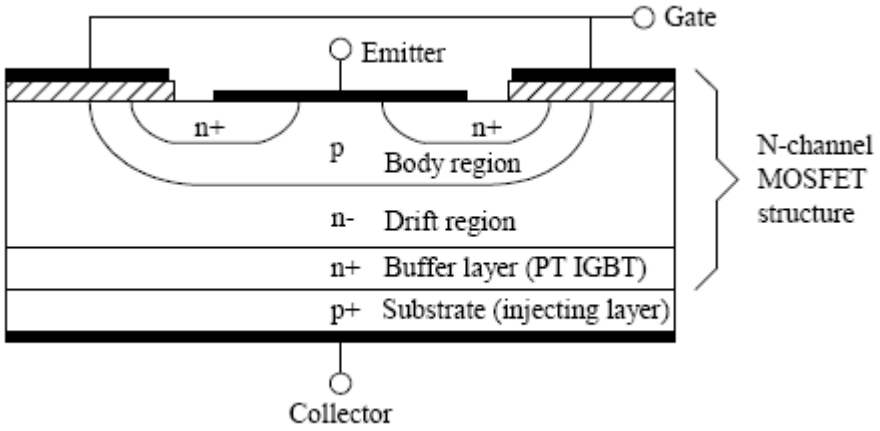

Fig. 2.26: N-channel IGBT cross-section

The flow of electrons draws positive ions, or holes, from the p-type substrate into the drift region toward the emitter. This leads to a couple of simplified equivalent circuits for an IGBT as shown in Fig. x. The first circuit shows an N-channel power MOSFET driving a wide base PNP bipolar transistor in a Darlington configuration. The second circuit simply shows a diode in series with the drain of an N-channel power MOSFET.

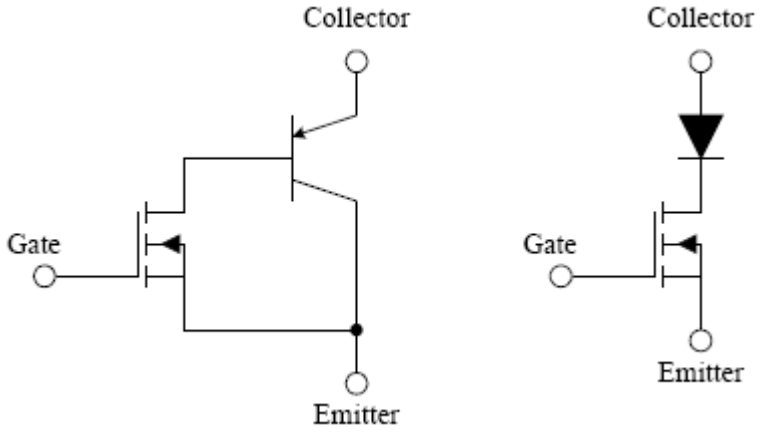

Fig. 2.27: IGBT simplified equivalent circuits

2.8.2.1 PT versus NPT Technology

The IGBT exhibits a tail current during turn-off until all the holes are recombined. The rate of recombination can be controlled, which is the purpose of the n+ buffer layer shown in Fig. 2.26. This buffer layer quickly absorbs trapped holes during turn-off. Not all IGBTs incorporate an n+

buffer layer; those that do are called Punch-Through (PT), those that do not are called Non Punch-Through (NPT). PT IGBTs are sometimes referred to as asymmetrical, and NPT as symmetrical.

- For a given switching speed, NPT technology generally has a higher V_{CE}(on) than PT technology. This difference is magnified further by fact that V_{CE}(on) increases with temperature for NPT (positive temperature coefficient), whereas V_{CE}(on) decreases with temperature for PT (negative temperature coefficient).

- For a given V_{CE}(on), PT IGBTs have a higher speed switching capability with lower total witching energy. This is due to higher gain and minority carrier lifetime reduction, which quenches the tail current.

- NPT IGBTs are typically short circuit rated while PT devices often are not, and NPT IGBTs can absorb more avalanche energy than PT IGBTs. NPT technology is more rugged due to the wider base and lower gain of the PNP bipolar transistor. This is the main advantage gained by trading off switching speed with NPT technology.

- For both PT and NPT IGBTs, turn-on switching speed and loss are practically unaffected by temperature. Reverse recovery current in a diode however increases with temperature, so temperature effects of an external diode in the power circuit affect IGBT turn-on loss.

2.7.3 Parallel Switched MOSFET with IGBT

This is an old idea that is reviving because the advanced power module technology in connection with elevated requirements for efficiency makes the utilization economical.
This combination leads to two basic improvements:

1. Boosting of efficiency at the high load range by rendering the static losses of the switch to the IGBT and the dynamic losses to the MOSFET.

2. Boosting of efficiency at light load range by rendering both the static and the switching losses to the MOSFET.

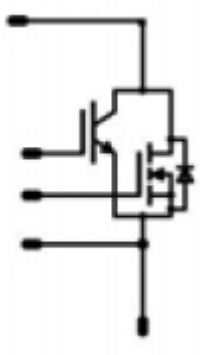

Fig. 2.28: MOSFET in parallel with IGBT

The MOSFET turns on fast and is delayed at switch off. It will also carry the current at low power so eliminating one p-n junction voltage drop of the IGBT whereas the IGBT will take the majority at max load condition. At low load the IGBT is not conducting at all so residual tail current losses are eliminated for the whole power range. With this topology it is possible to improve both the overall and the maximum load efficiency (Frisch *et al*, 2008).

2.9 Commercial Inverters

For better understanding of the reality of the “inverters world” it is presented in the table 2.1 various models of inverters of the three leader manufactures, the SUNGROW, the SUNNY BOY and ENPHASE. This table features these inverters according to their input and output range of voltage, current and power, their performances and efficiencies. All the data exposed was taken from their respective datasheets.

Table 2.1: Characteristics of some commercial inverters

Commercial inverters	Max. DC Power	Max. DC voltage	Max. DC current	Max. output power	MPPT	Power Transf.	Max. efficiency	CEC efficiency
SUNGROW								
SG10KTL	10.4 kW	1000 V	40 A	10 kW	Yes	No	98.0%	97.2%
SG2K5TL	2.8 W	450 V	15 A	2.5 kW	Yes	No	95.0%	94.5%
SG1K5TL	1.7 kW	450 V	12 A	1.5 W	Yes	No	95.0%	94.5%
SUNNY BOY								
3000TL	3.2 kW	550 V	17 A	3.0 kW	Yes	No	97.0%	96.0%
2000HF	2.5 kW	600 V	12.2 A	2.0 kW	Yes	Yes (HF)	96.0%	95.0%
700-US	575 W	150 V	7 A	460 W	No	Yes (LF)	92.4%	91.5%
ENPHASE MICROINVERTER								
D380	230 W	56 V	10A	380W	Yes	No	95.5%	95.0%
M210	240 W	62 V	10A	210 W	Yes	No	99.6%	95.5%
M190	230 W	56 V	10 A	190 W	Yes	No	99.6%	95.0%

Chapter 3

Simulation of different topologies in MatLab-Simulink

Nowadays, the simulation softwares are a great help on the development of products in so many areas of engineering. With them, the development became much more practical and less costly. This chapter presents simulations of some solutions for a low power inverter for photovoltaic systems using the MatLab-Simulink program.

3.1 PWM pulse generator

The following diagram block is built to generate PWM pulse used to control the switching of the MOSFETs used in the inverter circuits. A simple method to generate the PWM pulse train corresponding to a given signal is the interceptive PWM: a sine wave is compared with a sawtooth waveform. When the latter is less than the former, the PWM signal is in high state (1). Otherwise it is in the low state (0).

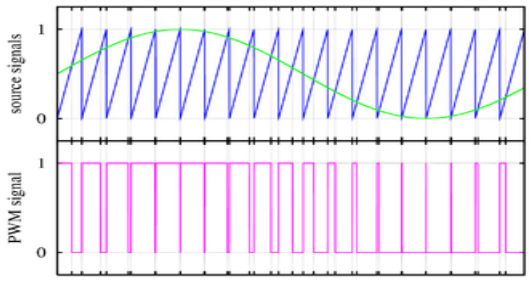

Fig. 3.1: PWM signal

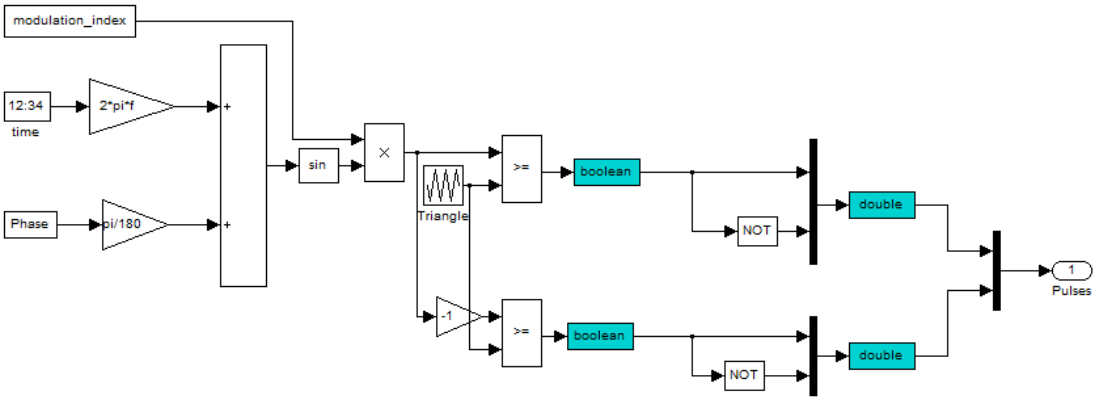

Fig. 3.2: PWM generation

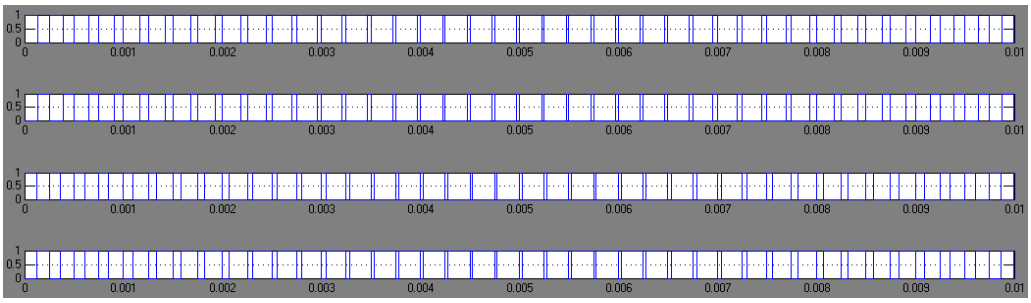

Fig 3.3: PWM pulses

3.2 PWM inverter with LF transformer

This is a simple topology with a MOSFET H-bridge inverter and a linear transformer.

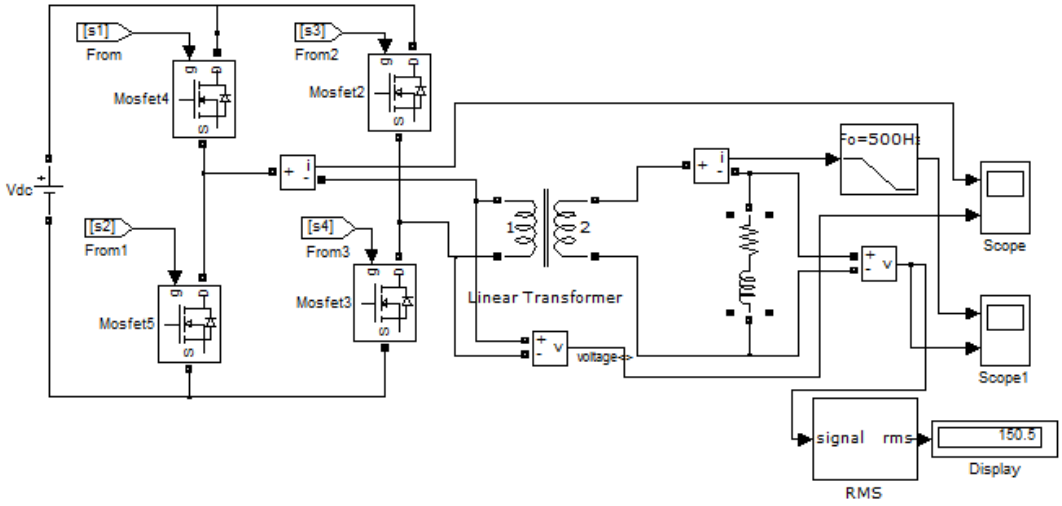

Fig. 3.4: PWM inverter with LF transformer

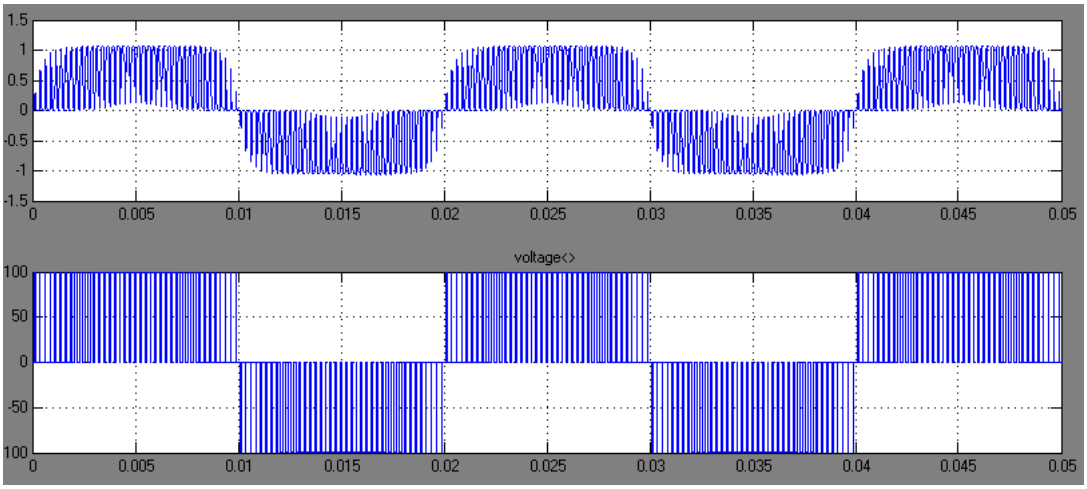

Fig. 3.5: signals on bridge output

The figure above shows us the how the H-bridge circuit creates an alternated waveform from a simple 100 V DC signal. To elevate the voltage there is the transformer and a filter to improve the quality of the current (fig.3.5).

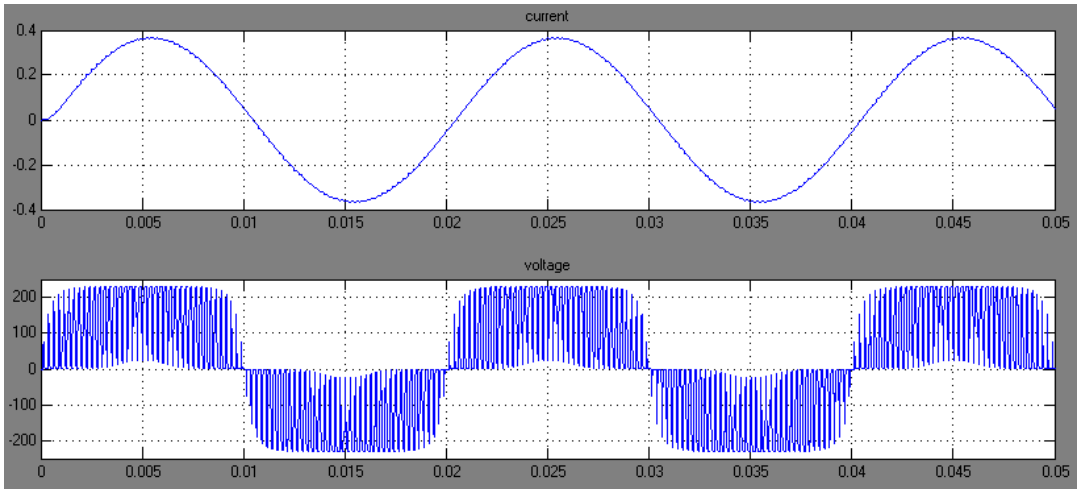

Fig. 3.6: output signals

Advantages:

- Simplicity in the design and control
- Galvanic isolation
- Symmetric sine wave

Limitations:

- The need of a transformer
- Weightier product

3.3 PWM inverter with boost

This system adds a boost to an H-bridge DC/AC converter to elevate the output voltage.

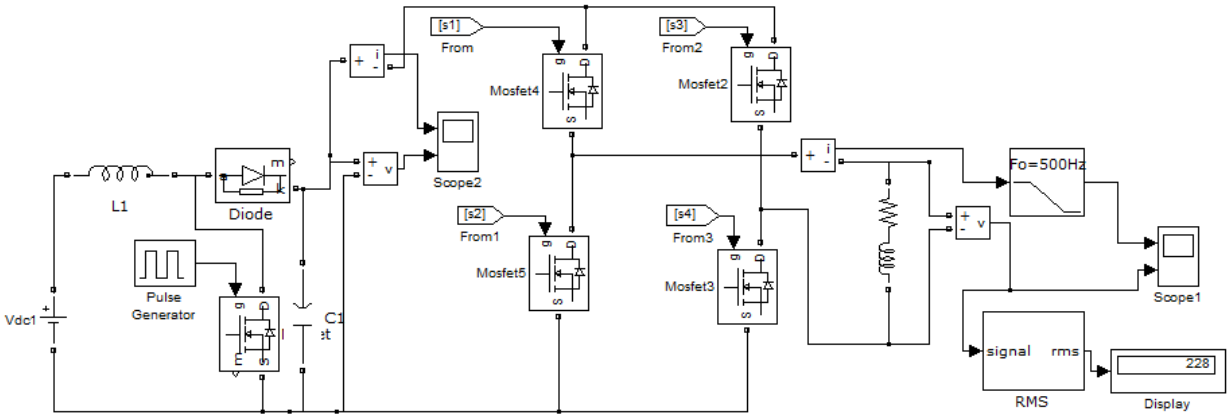

Fig. 3.7: PWM inverter with boost

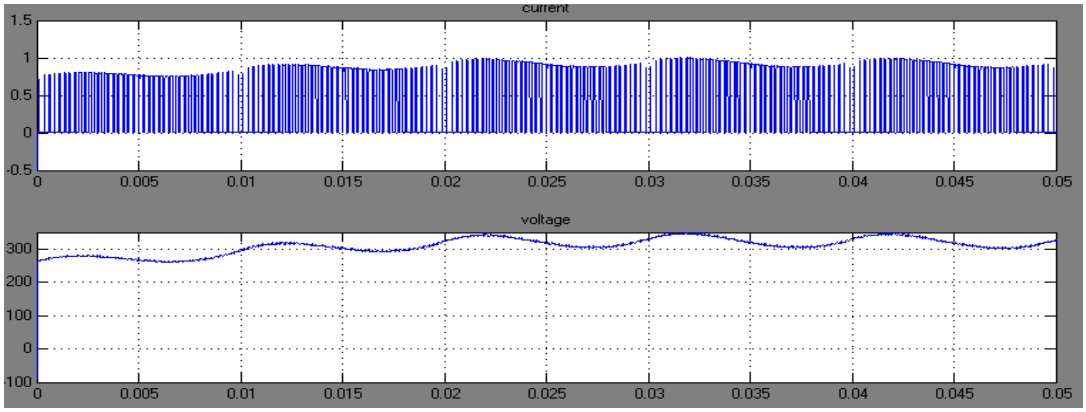

Fig. 3.8: signals on boost output

In the fig. 3.8 we have the boost output where the DC voltage is elevated until a reasonable value in order to have a 230 V AC voltage output (fig.3.9).

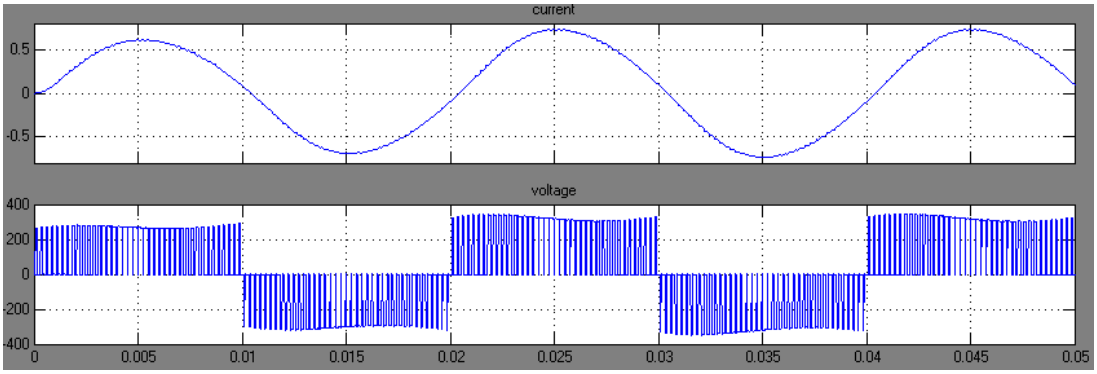

Fig. 3.9: output signals

Advantages:

- Exemption of transformer
- Lighter product
- Output voltage control

Limitations:

- Complex design and control
- No galvanic isolation
- Initial transitory

3.4 PWM inverter with Boost and Transformer

This system adds a boost and a LF transformer to an H-bridge DC/AC converter to elevate the output voltage.

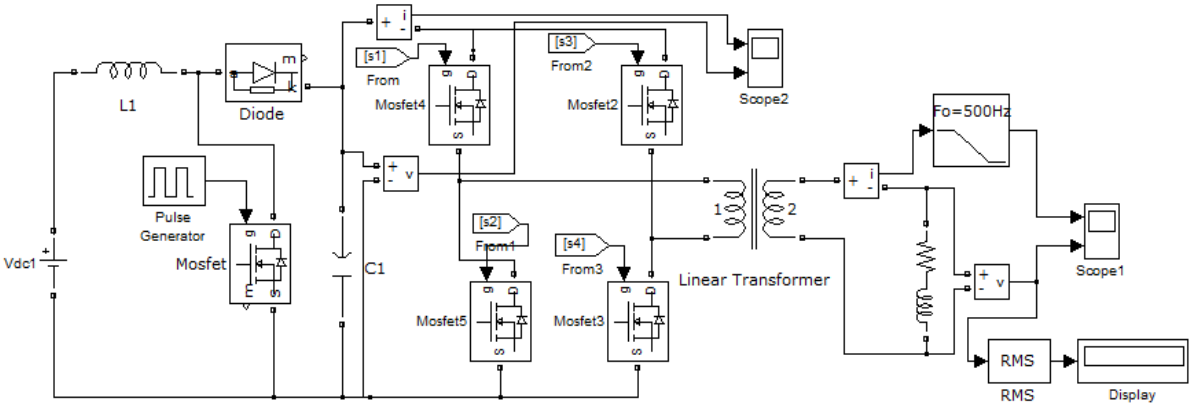

Fig. 3.10: PWM inverter with boost and LF transformer

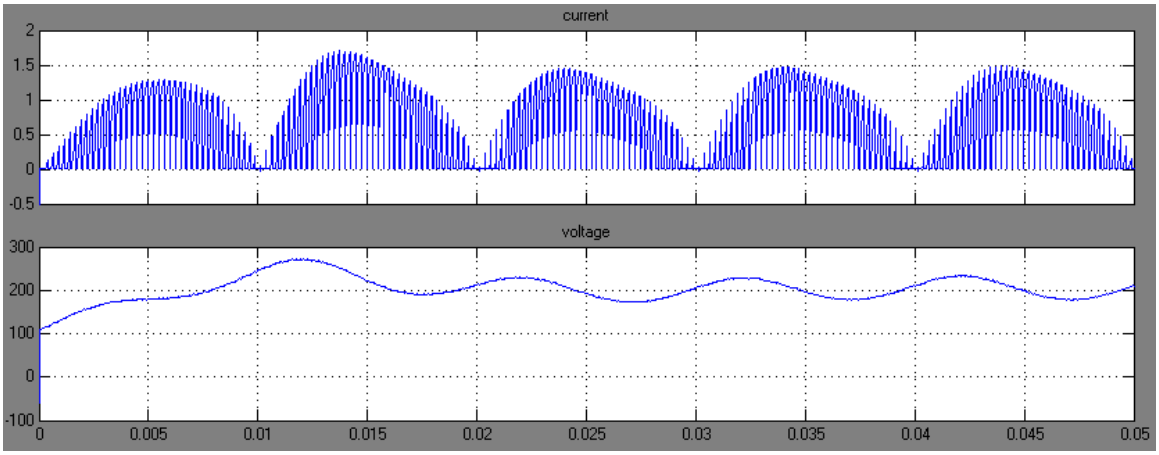

Fig. 3.11: signals on boost output

As you can see in the fig. 3.11, the level of the voltage elevation is less than the one shown in the fig. 3.8 corresponding to the anterior solution once there is a transformer to help the adjustment.

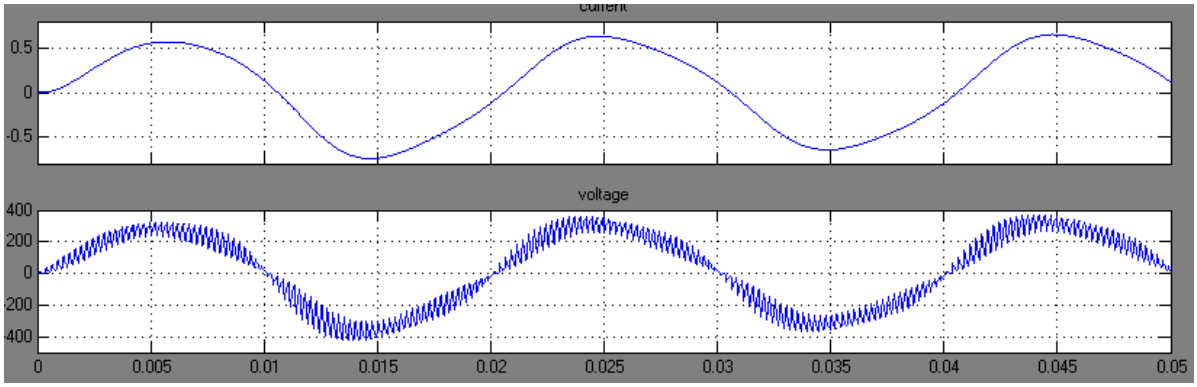

Fig. 3.12: output signals

Advantages:

- Output voltage control
- Galvanic isolation
- Mppt implementation possibility

Limitations:

- More complex circuits
- Complex control
- Initial transitory

3.5 5-level inverter

A multi-level inverter is especially used when high level of current is required and the switching frequency capability of the devices is low.

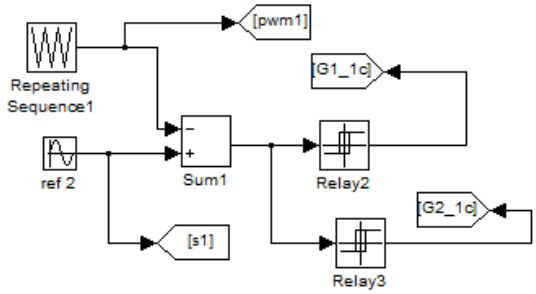

Fig. 3.13: PWM control for multi-level inverter

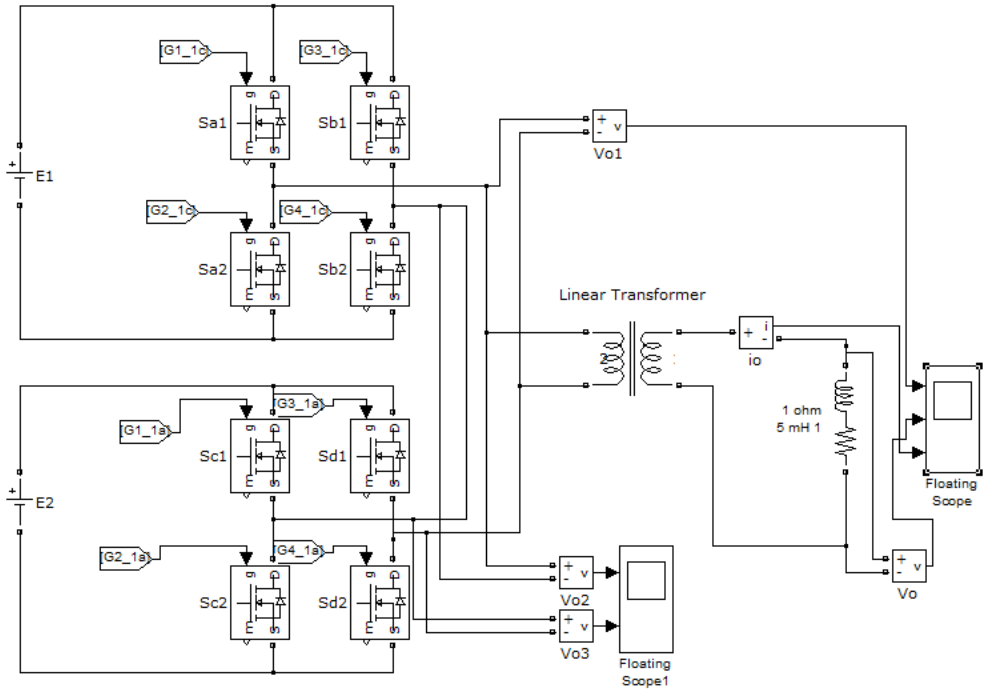

Fig. 3.14: 5-level inverter

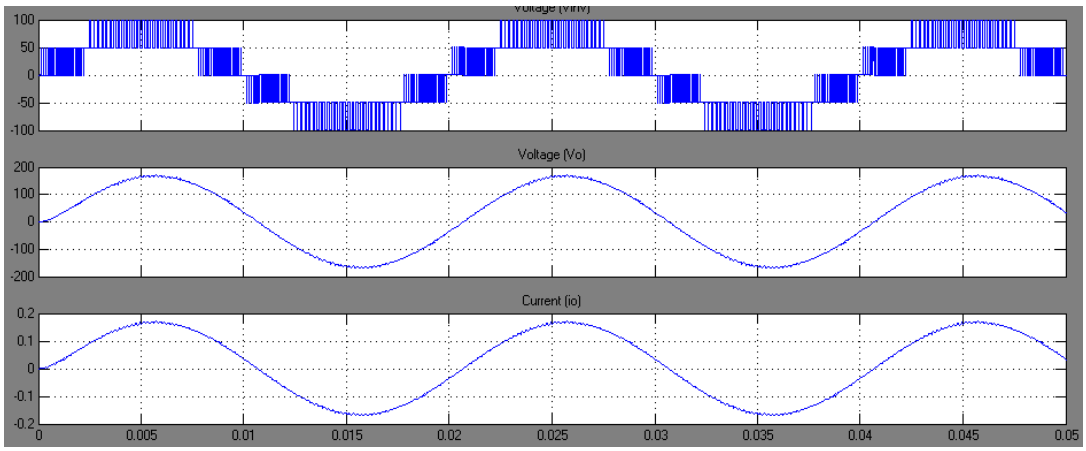

Fig. 3.15: Output signals

The first graph of the fig. 3.15 represents the 5 level of voltage resulting of the algebraic sum of the two 50 V input DC voltage in different period of time (-100V, -50V, 0V, 50V, 100V). There is the need to use a transformer once within this topology it is difficult to have the output voltage at grid's level. The transformer helps to filter the current as well.

Advantages:

- Lower switching frequency
- Higher quality sine wave
- Galvanic isolation

Limitations:

- Complex circuits design
- Complex control
- Use of more number of switching devices
- Need of transformer

3.6 Inverter topology selection

Table 3.1 contains a qualitative comparison between the different simulated inverter topologies related above. These comparisons are done according to features like the circuits and control complexity, the reliability, adaptability in different work conditions, the output signal quality, the insolation from the grid discharge, global weight and cost-effectiveness.

Table 3.1: Comparison between different topologies (+++ Very Good, ++ Good, + Bad)

	Circuits simplicity	Control simplicity	Reliability	Adaptability	Signal quality	Galvanic isolation	Weight	Cost effective
DC/AC-transformer	+++	+++	++	+	++	+++	+	++
Boost-DC/AC (transformerless)	++	++	+++	+++	++	+	+++	++
Boost-DC/AC-transformer	++	++	+++	+++	++	+++	+	++
5 level inverter-transformer	+	+	+++	+	+++	+++	+	+

After analyzing every aspects of each simulated topology as the simplicity of the project implementation, the reliability on field, the adaptability of working in different conditions, the quality of the output signal, weight and specially the cost, the solution where we have a DC/DC boost converter followed by a H-bridge IGBT inverter and LF transformer is the most promising. The presence of the transformer of this topology results in an increase of cost, power losses and global weight and volume, but it provides a good filtering of the current and galvanic insolation from the grid which protects the device. Also, the output results of other topologies simulated, fig.3.6, 3.9 and 3.15, reveals that it is quite difficult to elevate the voltage from the module range to grid network levels. This is the main reason of choosing the topology previously mentioned. This kind of inverter is usually kwon as two-stage single-phase inverter.

Chapter 4

The Two-Stage Single-Phase Inverter

4.1 Module scale two-stage single-phase inverter

After some comparisons between the various inverter topologies through theory analysis and practical simulations in Simulink, it comes to the conclusion that the most appropriate topology for this case of study should be a two-stage inverter due to its good reliability, facility of control and the quality of the output signal. This topology is composed by two main electronics blocks, the DC-DC converter and a DC-AC inverter, controlled independently as shown in the fig. 4.1.

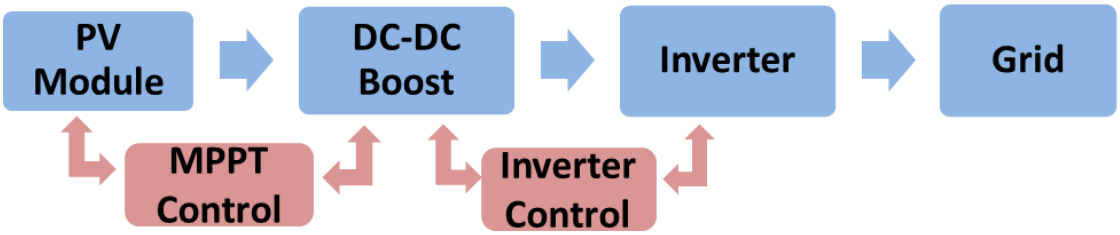

Fig. 4.1: Two-stage Inverter diagram

To carry out the whole project it is used, once again, the Simulink platform to create a model for a PV module, a boost converter, an IGBT full bridge inverter, a power transformer and grid line. By integrate them within respective control system it is provided a good image of what is going to be the real equipment.

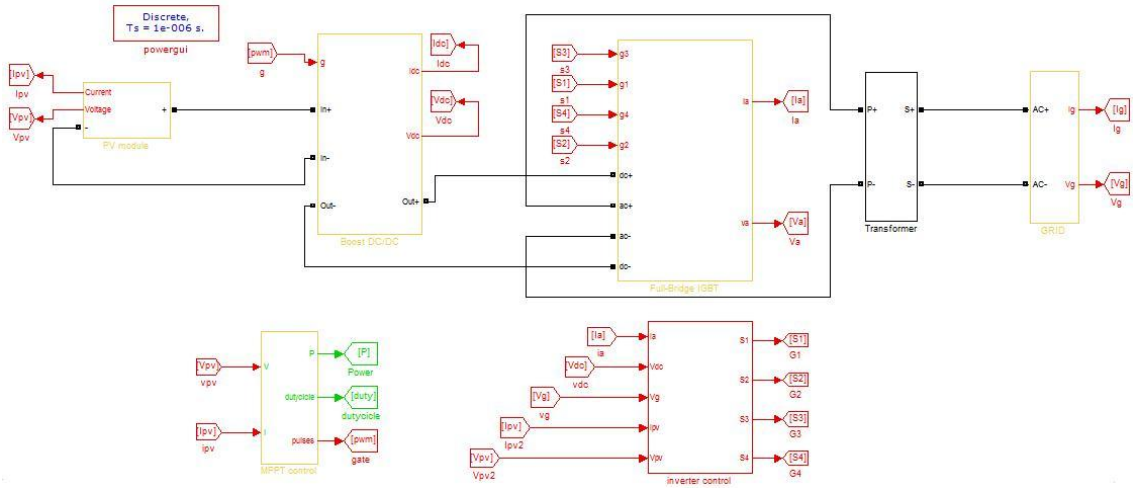

Fig. 4.2: Simulink project implementation

4.2 PV module equivalent circuit

The photovoltaic modules are made up of silicon cells. The silicon solar cells which give output voltage of around 0.7 V under open circuit condition. When many such cells are connected in series we get a solar PV module. The current rating of the modules depends on the area of the individual cells. Higher the cell area high is the current output of the cell.

The PV module modulation was made based on the typical simplified equivalent circuit of a PV cell (fig. 3), driven by the parameters shown in the block parameters in fig. 4.4.

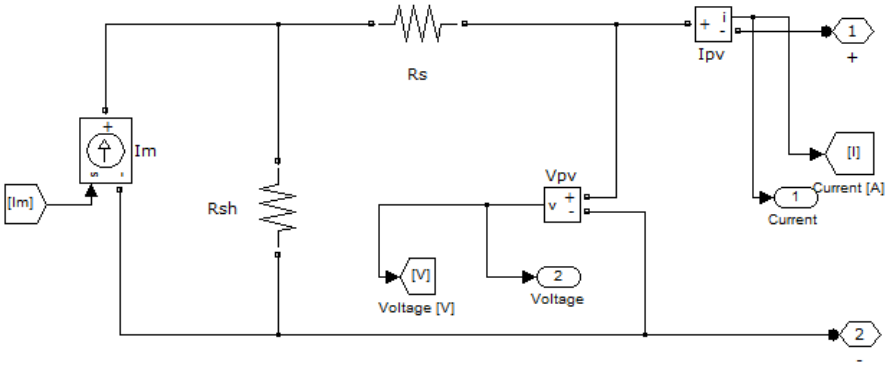

Fig.4.3: PV cell modulation in Simulink

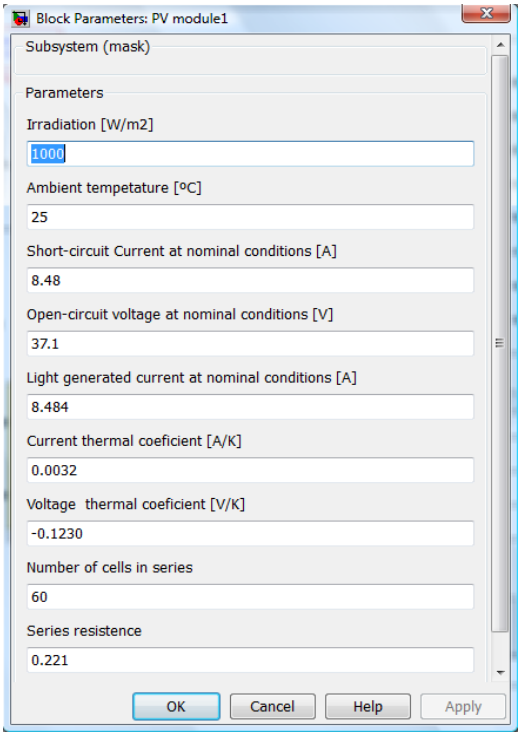

Fig.4.4: Block Parameters of the PV module

A typical characteristic of current (I) and voltage (V) curve and power (P) and voltage (V) curve of the module is shown is shown in fig. 4.5.

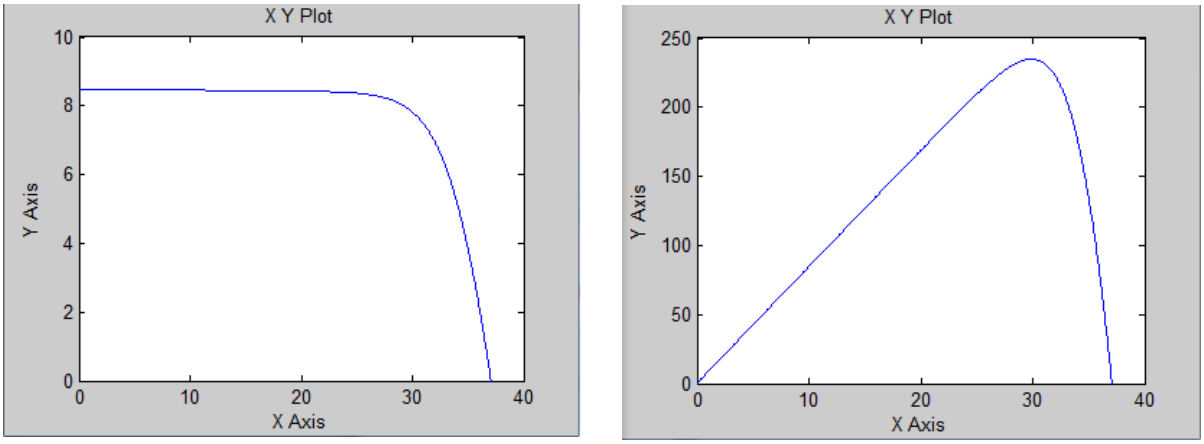

Fig. 4.5: Current-Voltage and Power-Voltage Curves of the PV module at NTC conditions (*Ir=1000 W.m^{-2} and Ta=25 ºC*).

4.3 DC/DC Boost Converter

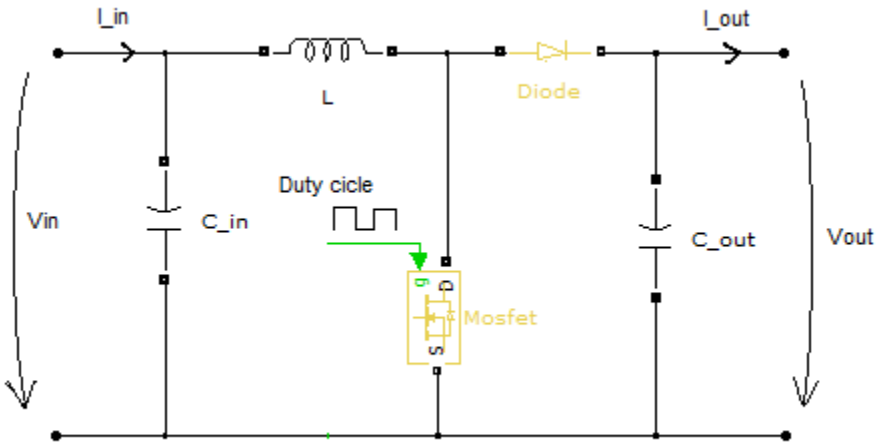

Fig. 4.6: Electric circuit of boost converter

4.3.1 Boost dimensioning

Table 4.1: Income values for boost dimensioning

Input nominal voltage – V_{in}	41.3 V
Input nominal current – I_{in}	5.1 A
Output voltage – V_{out}	200 V
Frequency of commutation – F_s	10 kHz

Duty-cycle (D)

Let's ignore the voltage drops on diode and transistor. During the time interval in which the switch leads, the inductor loads.

$$L * \frac{dI_{in}}{dt} = V_{in} \tag{1}$$

Or,

$$V_{in} = L * \frac{\Delta I_{in}}{T_{on}} = L * \frac{\Delta I_{in}}{DT} \tag{2}$$

During the time interval when the switch is open, the energy of the inductor and supply are both transferred to the load.

$$L * \frac{dI_{in}}{dt} = V_{in} - V_{out} \tag{3}$$

Or,

$$V_{in} - V_{out} = -L * \frac{\Delta I_{in}}{T_{off}} = -L * \frac{\Delta I_{in}}{(1-D)T} \tag{4}$$

Since the ripple current tour *ΔIin* are equal in driving and extinction conditions, comes,

$$\frac{DT * V_{in}}{L} = \frac{(1-D)T}{L}(V_{in} - V_{out}) \tag{5}$$

So,

$$V_{out} = \frac{V_{in}}{1-D} \tag{6}$$

$$1 - D = \frac{V_{in}}{V_{out}} \tag{7}$$

$$D = 1 - \frac{V_{in}}{V_{out}} \tag{8}$$

$$D = 1 - \frac{40}{200} = 0.8 \tag{9}$$

$$T = \frac{1}{F_s} \tag{10}$$

$$T_{on} = D * T = 8 * 10^{-5}\ \text{s} \tag{11}$$

$$T_{off} = (1 - D)T = 2 * 10^{-5} \text{ s} \tag{12}$$

$$L = \frac{(V_{in} - V_{out}) * T_{off}}{\Delta I_{in}} \tag{13}$$

For an input current ripple of 2.5% we have,

$$\Delta I_{in} = 0.025 * 5.1\ A = 0.13\ A \tag{14}$$

$$L = \frac{200 - 40}{0.13} 2 * 10^{-5} = 24.6\ mH \tag{15}$$

If we assume that every component of output ripple current ΔI_{out} passes through the capacitor C_{out}, and its average value I_{out} flows to the load, It comes,

$$\Delta V_{out} = \frac{\Delta Q}{C_{out}} \tag{16}$$

$$\Delta V_{out} = \frac{I_{out} * T_{on}}{C_{out}} \tag{17}$$

$$C_{out} = \frac{I_{out} * T_{on}}{\Delta V_{out}} \tag{18}$$

$$I_{out} = \frac{I_{in}}{k} \tag{19}$$

Where k is the voltage gain of the boost.

$$k = \frac{Vout}{Vin}$$

(20)

$$C_{out} = \frac{1.02 * 8 * 10^{-5}}{5.0} = 16.3\ \mu\text{F}$$

(21)

For a *Vout* ripple of 2.5 %.

Inductor Current,

$$I_L = I_{in} = 5.1\ A \tag{22}$$

$$I_{Lmax} = I_{sc} = 5.6\ A \tag{23}$$

4.3.2 Boost Control

To control any DC-DC converter we need a pulsing signal to drive the transistor. In this project the kind of transistor chosen is a MOSFET. The boost converter is controlled by the Maximum Power Point Tracking (MPPT) algorithm. The MPPT algorithm varies the I-V curve till it finds the point where the power is at maximum and stays around it. There are many kind of MPPT algorithm. One of the most used algorithms for peak power tracking is the “Perturb and Observe” algorithm due to its simplicity and reliability. It’s based on the simple process of increment a little perturbation on the duty cycle and observes if the Power is rising up or going down. If it’s rising up the perturbation proceeds its way and if the power goes down the perturbation inverts the way. For better understanding of this algorithm it is presented its flowchart bellow.

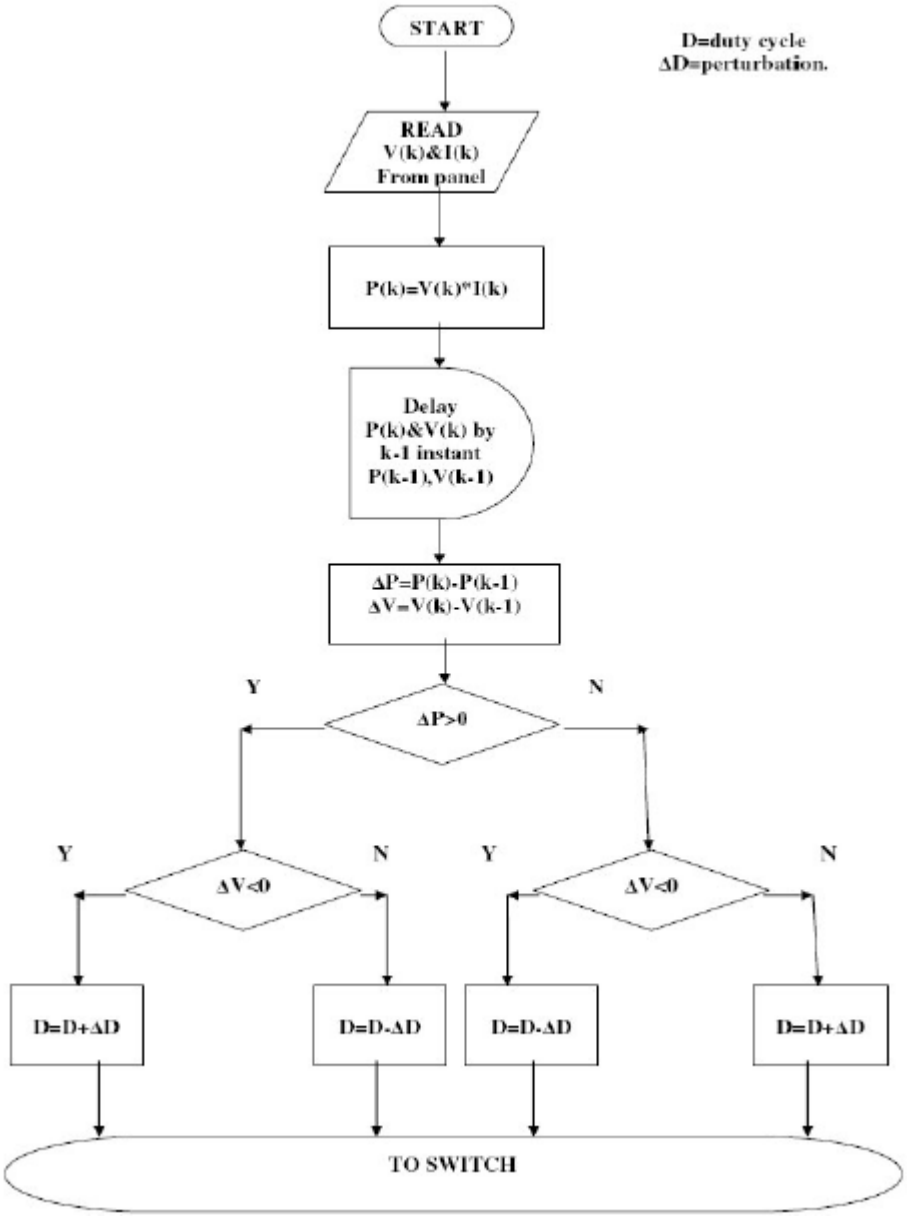

Fig. 4.7: Perturb and observe algorithm flowchart
From: CHAUDHARI, 2005

Following the flowchart above it is built the controlling algorithm in Simulink according as shown in fig. 4.8.

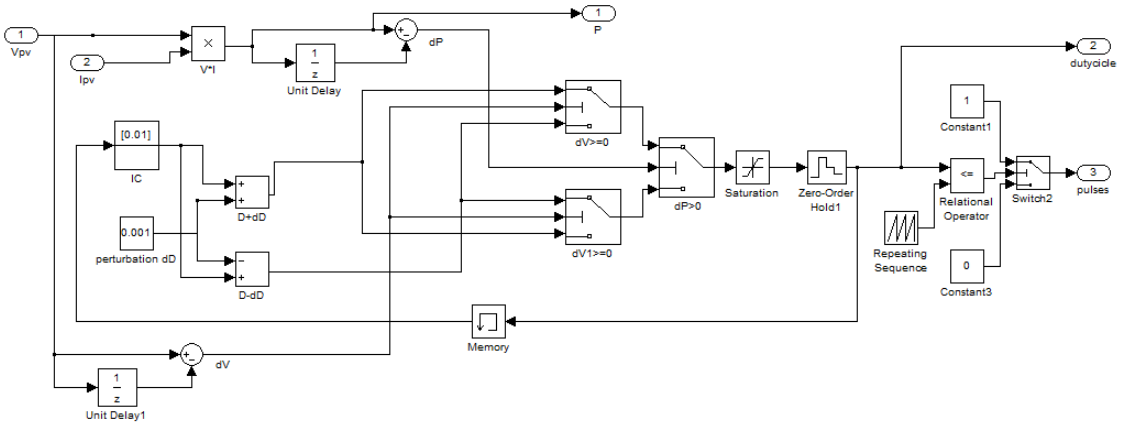

Fig. 4.8: Perturb and Observe MPPT algorithm in Simulink

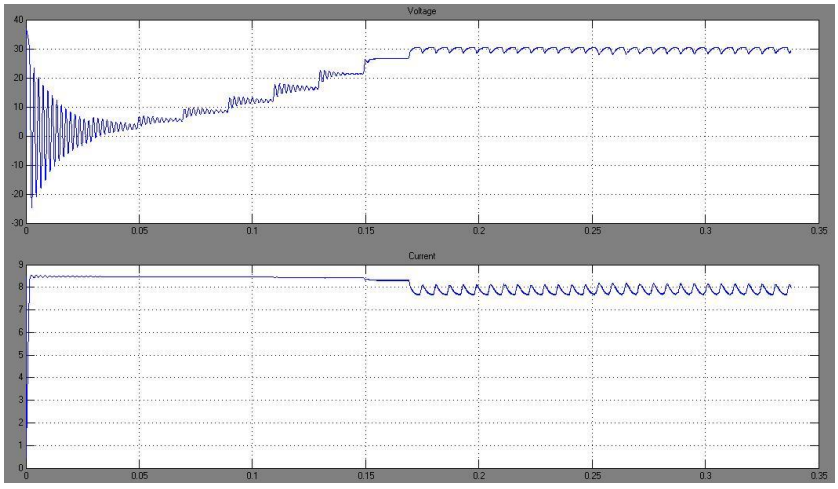

Fig. 4.9: Input Voltage and Current

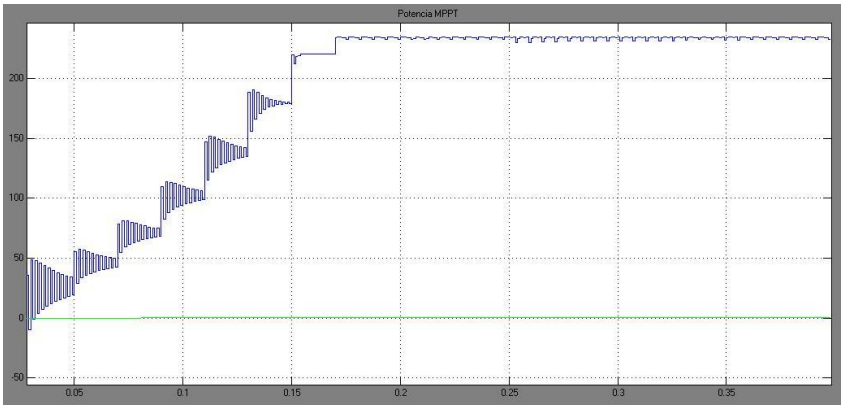

Fig. 4.10: Maximum Power Tracking

4.4 DC-AC Converter

For the DC to AC converter a full-bridge inverter from IGBTs module was used. Each IGBT arm from the module must support a voltage of 200 V that corresponds to the boost outputs.

4.4.1 Inverter control

In the inverter control system, it is used a Proportional-Integral (PI) closed loop control for the DC voltage control, and a fixed band bang-bang current control. The amplitude of the reference current is given by the estimative power production by the module and the phase and frequency are taken from the Phase-Loop-Lock (PLL).

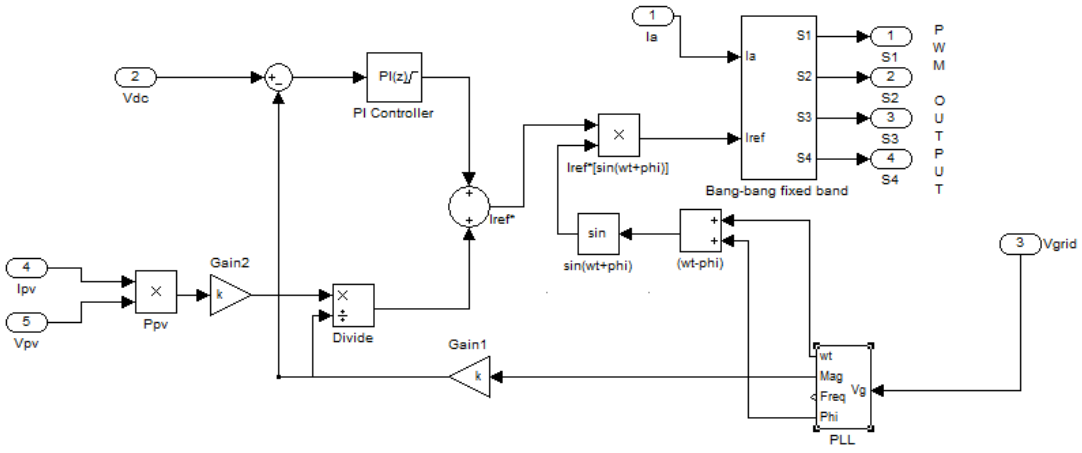

Fig. 4.11: Inverter control system

4.4.1.1 PLL control

Phase, amplitude and frequency of the utility voltage are critical information for the operation of the grid-connected inverter systems. In such applications, an accurate and fast detection of the phase angle, amplitude and frequency of the utility voltage is essential to assure the correct generation of the reference signals and to cope with the new upcoming standards.

The main task of a PLL structure is to provide a unitary power factor operation, which involves synchronization of the inverter output current with the voltage, and to give a clean sinusoidal current reference. Also using a PLL structure the grid voltage parameters, such as amplitude and frequency can be monitored (Ciobotaru et all, 2006).

The general structure of a single-phase PLL including the grid voltage monitoring is shown in the fig. 4.12.

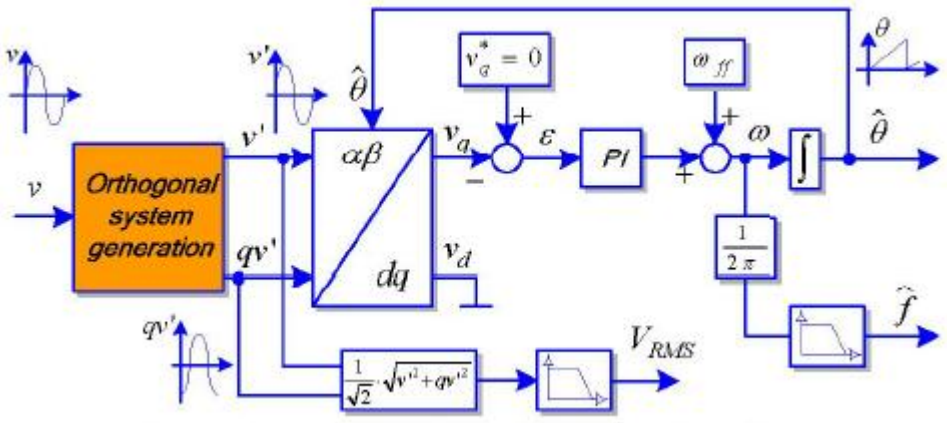

Fig. 4.12: General structure of single-phase PLL
From: Ciobotaru *et al,* 2006

For the simulation purpose it is used the single-phase PLL block from the Simulink library, but for the implementation it is built a C code based on the structure of the fig. 4.12.

4.4.1.2 PI controller of DC-link voltage

To regulate the DC-link voltage and the output current it is used a feedback PI controller. The PI controller calculates an ‘‘error’’ value as the difference between a measured DC-link voltage and a desired setpoint voltage in a closed loop system. The transfer function of the PI controller is given by:

$$Gpi(s) = Kp + \frac{Ki}{s} \tag{24}$$

4.4.1.3 Bang-bang current control

A variety of current controlled techniques have been studied and reported in the literature. They are classified as linear and non-linear current controllers. Linear controller, including PI controller, state feedback controller and predictive current controller, requires the complete knowledge of load parameters and it needs more calculation. Therefore, non-linear controller includes bang-bang controllers (Hysteresis control, ramp type control and delta modulator) and

predictive controllers with online-optimization and does not need the load information and it provides good dynamic response to the system.

The hysteresis band current control is used very often because of its simplicity. Besides fast response current loop, the method doesn't need any knowledge of load parameters. But it has the disadvantage that the switching frequency is irregular and current ripple is relatively large. The hysteresis band can be programmed as a function of load and supply parameters in order to maintain a fixed modulation frequency. There are two kinds of hysteresis band control: The fixed band and the sinusoidal band.

In fixed band, the hysteresis band is fixed whereas in sinusoidal band the hysteresis bands vary over a fundamental period. The fixed-band hysteresis controller gives good performance except that the switching frequency is irregular and current ripple is relatively large. But in a sinusoidal band hysteresis current controller, the ripple can be varied with the current magnitude thereby reducing the current ripple content. So a lesser ripple would result in a lower harmonic content keeping, in fact, the fast response and simplicity of implementation of hysteresis current controllers (Mohapatra and Babu, 2010).

Fixed Band Hysteresis

In this scheme, the hysteresis bands are fixed throughout the fundamental period. The algorithm for this scheme is given as:

$I_{ref} = I_{max} * sin(\omega t)$

Upper band, $I_{up} = I_{ref} + h$

Lower band, $I_{low} = I_{ref} - h$

Where h = Hysteresis band limit

If $I_a > I_{up}$, $V_{ao} = - V_{DC}/2$
If $I_a < I_{low}$, $V_{ao} = + V_{DC}/2$

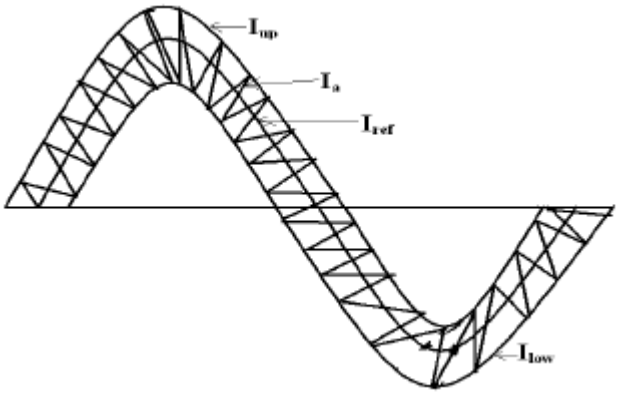

Fig. 4.13: fixed band hysteresis
From: Mohapatra and Babu, 2010

Sinusoidal Band Scheme

In this scheme, the hysteresis bands vary sinusoidally over a fundamental period. The upper and lower bands are given as:

$I_{ref} = I_{max} * sin(\omega t)$

Upper band, $I_{up} = (I_{max} + h)sin(\omega t)$

Lower band, $I_{low} = (I_{max} - h)sin(\omega t)$

The algorithm is given as follows:

For $I_{ref} > 0$:

If $I_a > I_{up}$, $V_{ao} = -V_{DC}/2$

If $I_a < I_{low}$, $V_{ao} = +V_{DC}/2$

For $I_{ref} < 0$:

If $I_a < I_{up}$, $V_{ao} = +V_{DC}/2$

If $I_a > I_{low}$, $V_{ao} = -V_{DC}/2$

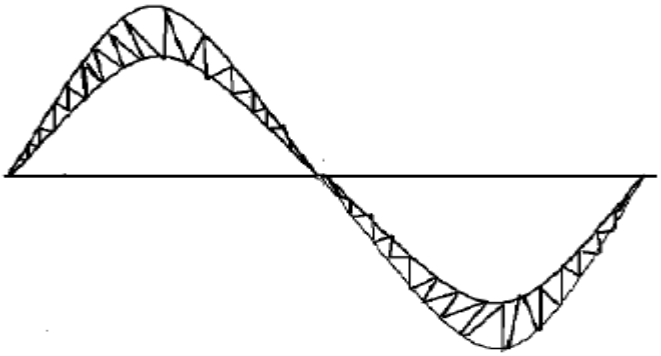

Fig. 4.14: Sinusoidal band Hysteresis
From: Mohapatra and Babu, 2010

One of the most critical parameters in this kind of bang-bang control is the Maximum Switching Frequency. According to the reference (Mohapatra and Babu, 2010) this parameter is given as:

$$MSF_{fixed} = \frac{f_m(SN + 2\pi M)}{4h} \tag{25}$$

And,

$$MSF_{sin} = \frac{f_m N}{2} \tag{26}$$

Where fm is the frequency of the reference current, S is the current increment in the sampling interval, N is the sampling rating per cycle and M is the peak value of sine wave.

The Maximum Switching Frequency is more critical for the sinusoidal band hysteresis control (), so I chose to use fixed band control in the simulation and physical implementation once the frequency of commutation is a critical limitation of the devices.

In the fig. 4.15 and fig. 4.16 you can see the scope of the simulation result of this controlling type.

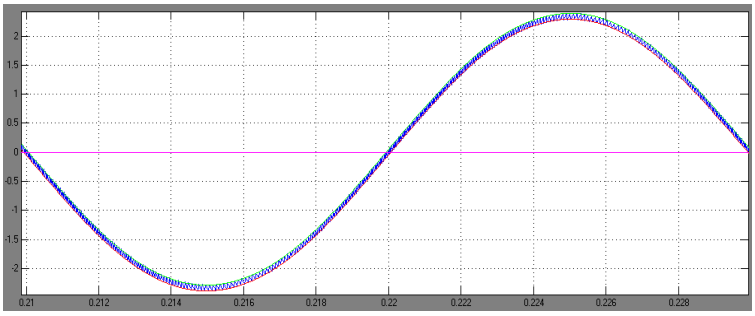

Fig. 4.15: Bang-bang current control

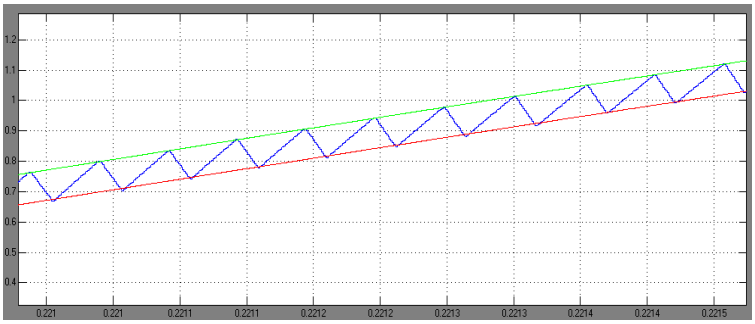

Fig. 4.16: Current zoom

4.5 Integrated Project Simulations

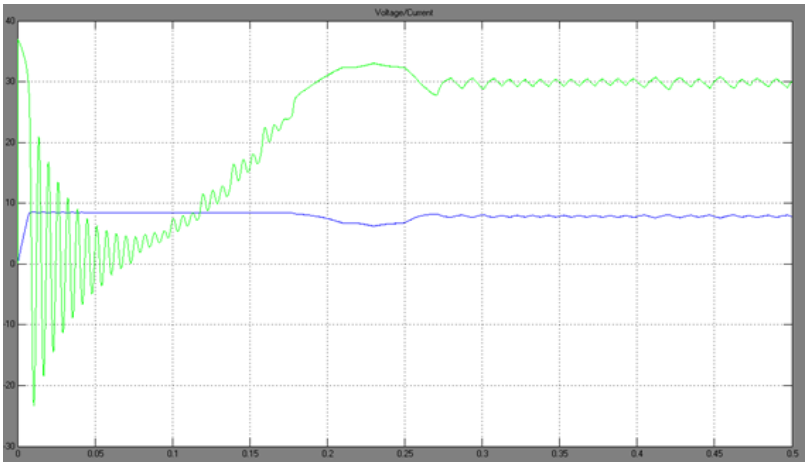

Fig. 4.17: Output Module Voltage and Current

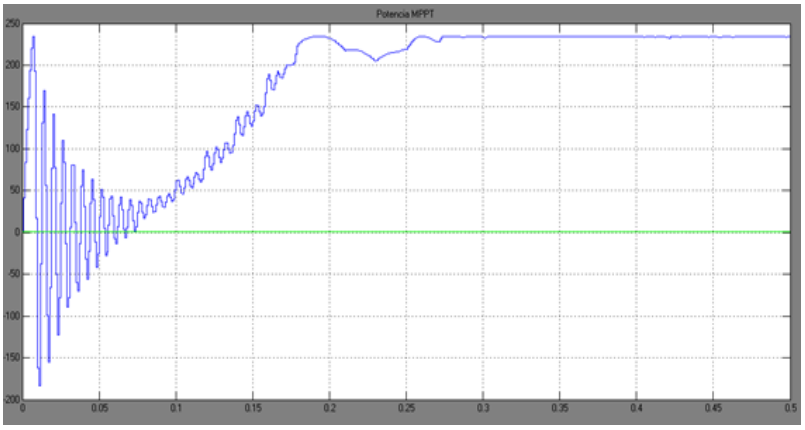

Fig. 4.18: Power delivered - MPPT

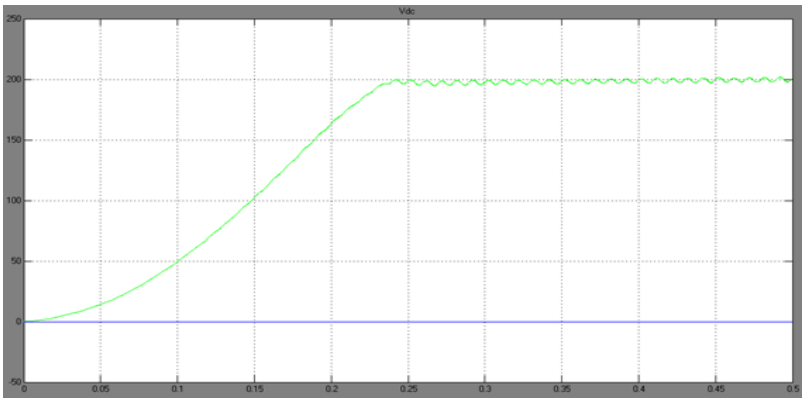

Fig. 4.19: Boost output DC Voltage

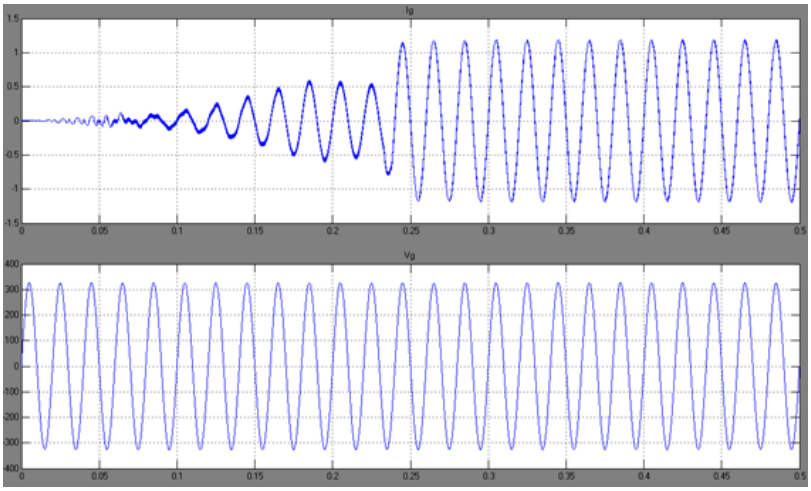

Fig. 4.20: Output Voltage and Current injected to the grid.

Chapter 5

Project Implementation and Tests

After all the calculus for the components dimensioning, they are purchased in the market to start the implementation. The implementation is stated with the boost elements assembling and tests. After that it was mounted the current and voltage sensors for the *Ipv* and *Vpv*, with their respective auxiliary electronics circuits. With the boost converter parts ready the Arduino board is placed on with the boost part control code upgraded. After good results of the boost testing the mounting is continued with the rest inverter parts and the respective control software is upgraded to the board. With the inverter ready, it is connected to the LF transformer and then available to make tests with PV module on the grid.

5.1 Arduino Uno Board

The control is done digitally using an Arduino Uno board. Arduino is an open-source physical computing platform based on a simple microcontroller board, and a development environment for writing software for the board. It can be used to develop interactive objects, taking inputs from a variety of switches or sensors, and controlling a variety of lights, motors, and other physical outputs.

The Arduino programming language is an implementation of Wiring, a similar physical computing platform, which is based on the Processing multimedia programming environment. The programming environment is easy to use for beginners, yet flexible enough for advanced users to take advantage of as well.

The Arduino software is published as open source tools, available for extension by experienced programmers. The language can be expanded through C++ libraries, and people wanting to understand the technical details can make the leap from Arduino to the AVR C programming language on which it's based.

The Arduino Uno is a microcontroller board based on the ATmega328 chip of Atmel. It has 14 digital input/output pins (of which 6 can be used as PWM outputs), 6 analog inputs, a 16 MHz crystal oscillator, a USB connection, a power jack, an ICSP header, and a reset button.

It contains everything needed to support the microcontroller; simply connect it to a computer with a USB cable or power it with a AC-to-DC adapter or battery to get started.

Table 5.1: Arduino Uno summary

Microcontroller	ATmega328
Operating Voltage	5 V
Input Voltage (recommended)	7-12 V
Input Voltage (limits)	6-20 V
Digital I/O Pins	14 (of which 6 provide PWM output)
Analog Input Pins	6
DC Current per I/O Pin	40 mA
DC Current for 3.3V Pin	50 mA
Flash Memory	32 KB (ATmega328) of which 0.5 KB used by bootloader
SRAM	2 KB (ATmega328)
EEPROM	1 KB (ATmega328)
Clock Speed	16 MHz

From: *www.arduino.cc.*, Sept. 5, 2011

For more information of Arduino board and Atmega328 chip consult the datasheets in the Arduino official website *www.arduino.cc*.

5.2 Current and voltage measurement

The measurements are the most critical part of the project. However, they are very necessary to collect information to control the circuits. It is important that the measurements could be done with a good accuracy, so better efficiency can be achieved at the end.

We have to take in account that analog input pins from the control board accept values from 0 to 5V, so every input signal must be converted to match with those limits.

We need to measure the current and voltage from the PV module, *Ipv* and *Vpv* respectively, to process the MPPT algorithm control, the DC-link voltage, *Vdc*, for its regulation the Current injected to the grid, *Ig*, and the grid voltage, Vg, for PLL control.

For the currents measurements I used TALEMA ASM-010 current sensors, which is easy to use, linear and relatively cheap. These sensors have a linear response of current between 0 and 12

A that provokes a drop of voltage of 0 to 40 mV on a 50 ohm resistor. This output signal must be amplified one hundred times to suite with analog input range. The amplifier circuit is shown in the fig. 5.1.

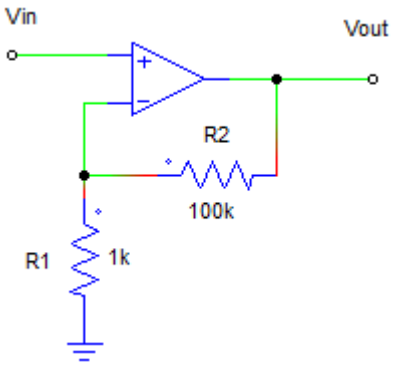

Fig. 5.1 Electronic amplifier circuit

Where,

$$V_{out} = \left(\frac{R2}{R1} + 1\right) * V_{in} \tag{27}$$

To Vpv and *Vdc* voltage measurements I used LEM voltage transducers that provide galvanic isolation between the high voltage circuit and electronic control circuit. These sensors are quiet expensive but they are necessary in order to avoid electric discharge and protect the microcontroller. The transducer must be connected according to the fig. 5.2.

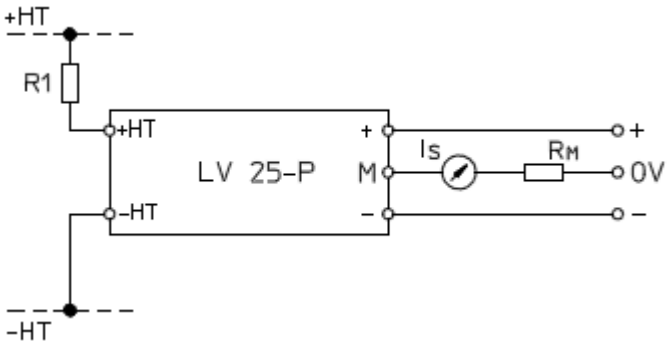

Fig. 5.2: Voltage transducer measurement scheme

A current proportional to the measuring voltage passes through the external resistor *R1 (28)*, which is selected according to the range of voltage to be measured. This resistor must be chosen so that the current is around 10 mA which offers accuracy of 0.8% of *Vpn* at *Tamb* of 25 ºC. The measurement resistor *Rm* (34) is chosen according to the range of voltage that the microcontroller accepts.

For the *Vpv* measurement we have,

$$R1 = \frac{V_{pn}}{I_p} \tag{28}$$

$$R1 = \frac{40\ V}{10 * 10^{-3} A} = 4k\Omega \tag{29}$$

Because of the market standards resistor I chose the 4.6 kΩ resistor.

I must also calculate the dissipation capability of the resistor, so

$$P_{R1} = \frac{2 * 40^2}{4.6 * 10^3} = 0.69\ W \tag{30}$$

Thereby, the chosen *R1* is a 4.6 kΩ of 1 W.

The current in the secondary I_s, is given as,

$$I_s = 2.5 * I_p \tag{31}$$

$$I_p = \frac{40}{4.6 * 10^3} = 8.69 * 10^{-3}\ A \tag{32}$$

$$I_s = 2.5 * 8.69 * 10^{-3} = 21.7 * 10^{-3}\ A \tag{33}$$

$$R_m = \frac{U_m}{I_s} \tag{34}$$

Where *Um* is the maximum voltage the ADC accepts.

$$R_m = \frac{5\ V}{21.7 * 10^{-3}\ A} = 230\ \Omega \tag{35}$$

$$P_{R_m} = 2 * \frac{5^2}{230} = 0.217\ W \tag{36}$$

So I chose the ¼ W 240 Ω resistor for R_m.

For DC-link voltage measurement the process is the same. So,

$$R1 = \frac{200\ V}{10 * 10^{-3}\ A} = 20\ k\Omega \tag{37}$$

$$P_{R1} = 2 * \frac{200^2}{20 * 10^3} = 4\ W \tag{39}$$

Thereby, I chose high power resistor with a rating of 5 W.

$$I_s = 2.5 * 10 * 10^{-3} = 25\ mA \tag{40}$$

$$R_m = \frac{5\ V}{25 * 10^{-3}\ A} = 200\ \Omega \tag{41}$$

$$P_{R_m} = 2 * \frac{5^2}{200} = 0.25\ W \tag{42}$$

On the other hand, the measurement of the grid voltage for PLL processing is made directly using voltage dividers. This method is risky for the Arduino analog input but once the grid voltage is normally stable it seems acceptable. The fig. 5.3 shows the Vg measurement circuits.

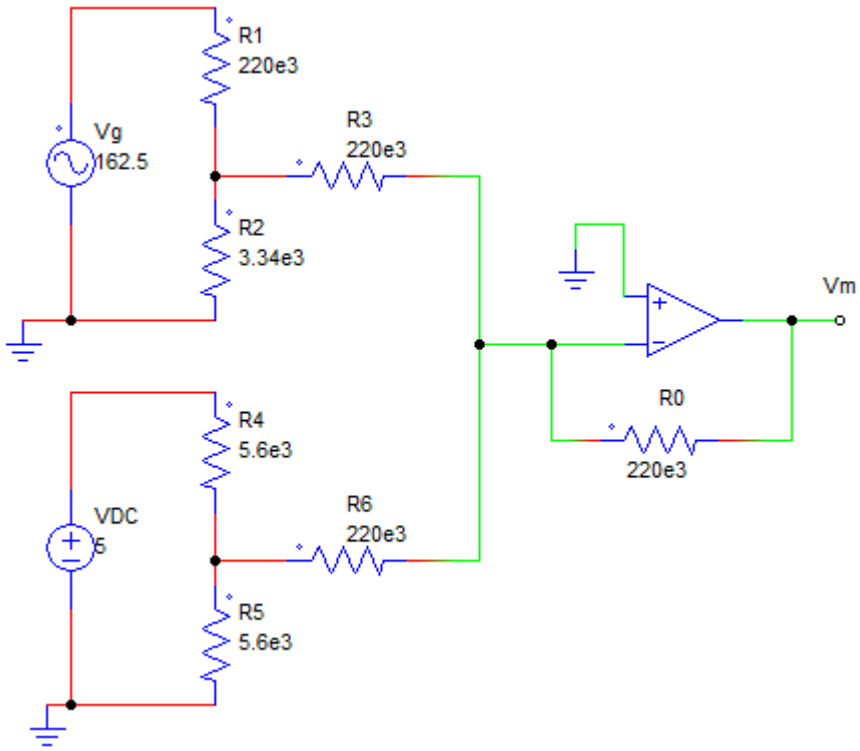

Fig. 5.3: Electronic circuit for Vg measurement

As the grid voltage after the transformer takes instant values between -162.5 V to 162.5 V, the first divider turns this voltage to values between -2.35 V to 2.35 V. the second divider, in turn, provides 2.5 V of 5 V. by adding these two voltages, using a operation amplifier adder circuit, we have the measuring voltage *Vm*, into a range between 0.15 V to 4.85 V with is in the range for the analog to digital converting.

For the V_g measurement the power dissipation is given by,

$$p = \frac{{V_g}_{rms}^{\,2}}{R_{eq}} \tag{43}$$

$$p = \frac{\left(\frac{162.5}{\sqrt{2}}\right)^2}{223 * 10^3} = 0.059\ W \tag{44}$$

So, the resistors used could be the standards ¼ watt.

5.3 Implementation

According to the calculations for the dimensioning of the components presented in the previous chapters, and its availability in the market, it follows in the Table 5.2 the list of materials chosen for the implementation of the prototype and their respective technical features.

Table 5.2: Materials and technical features

Components	Features	Voltage		Current		Part number
		Nom.	Max.	Nom.	Max.	
Inductor (1)	38mH				9.3A	8118-RC
Capacitors (2)	470uF	200V	200V			200VXG470MEFCSN25X30
	0.47uF	200V	200V			
Diode (3)			200V		8A	MUR820
IGBTs module (4)			600V		10A	STGIPS10K60A
Power transformer	250VA	115V/230V				
Current sensor (5)				1A - 10A	12A	ASM-010
Voltage sensor (6)		10V - 500V	500V	10mA		LV25-P
Microcontroller (7)	Arduino Uno (Table 5.1)					
Operational Amplifier						UA741
Voltage regulators	12V	12V				L7812CV
	24V	24V				L7824CV
Resistors	**1/4 W:** 47Ω, 200Ω, 230Ω, 1kΩ, 4.6kΩ, 5.6kΩ, 22kΩ, 220kΩ					
	1 W: 4.6 kΩ					
	5 W: 22kΩ					

The prototype is mounted in a board as it is shown in the picture of fig. 5.4. The legend in the prototype figure corresponds to the components in the table 5.2.

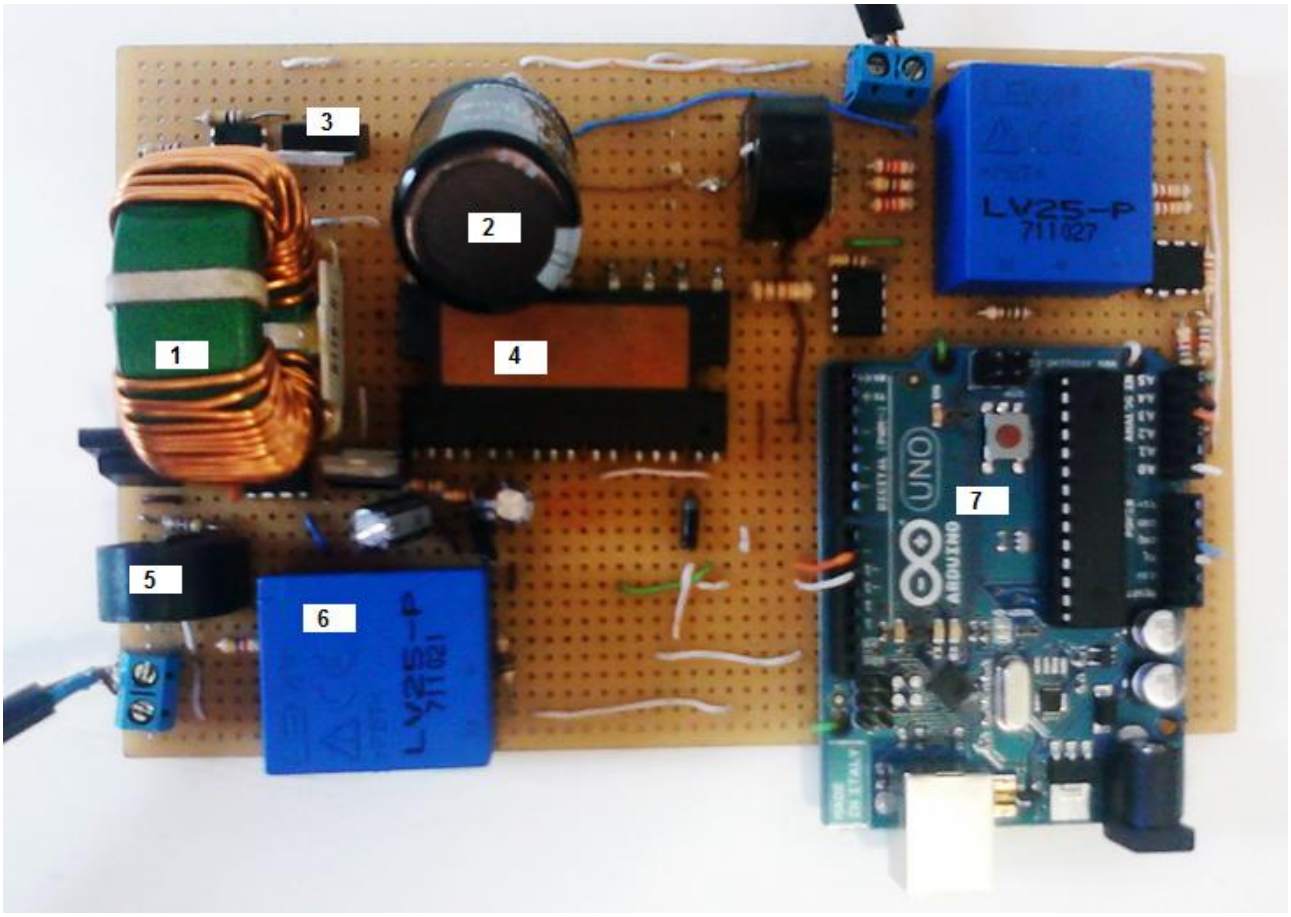

Fig. 5.4: Inverter prototype

5.4 Tests and results analysis

The final tests were done in a typical sunny day with the module properly oriented to the sun light. The PV module used for the tests has the features presented in the table 5.3.

Table 5.3: PV module features

Part number	HIP-210NKHA5
Pmax	210 W
Voc	50.9 V
Isc	5.57 A
Vmpp	41.3 A
Vmpp	5.09 A
Efficiency (η)	16.7%
Area (A)	1.28 m^2

For the test effect I created a virtual grid network and a physical resistive load to process the PLL and dissipate the energy. The network has a frequency of 50 Hz and 230 Vrms.

The critical parameters like V_{PV}, I_{PV}, V_{DC} and I_g, are read and processed by the Arduino microcontroller and then are transported to MatLab environment through the serial port at a rate of 9600 bps.

The fig. 5.5 and fig.5.6 represent the input of PV voltage and current respectively, read at the inverter input. The data were taken after the system had reached the steady state. The overage value of the voltage is 42.1 V with a ripple 4.8 V (11.4%), and current 3.8 A with a ripple of 0.4 A (10.5%). These ripples are due to the disturb-and-correct MPPT algorithm.

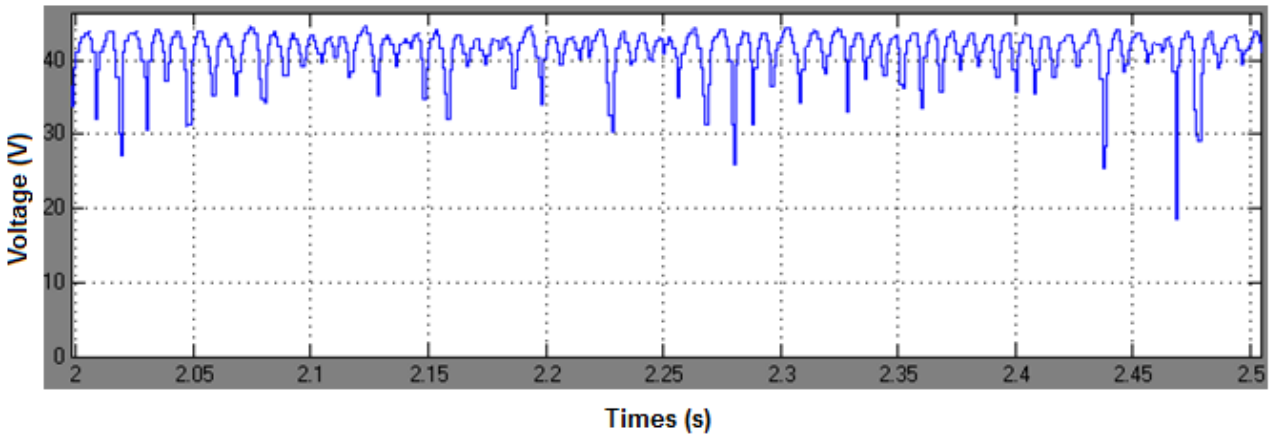

Fig. 5.5: Vpv acquisition

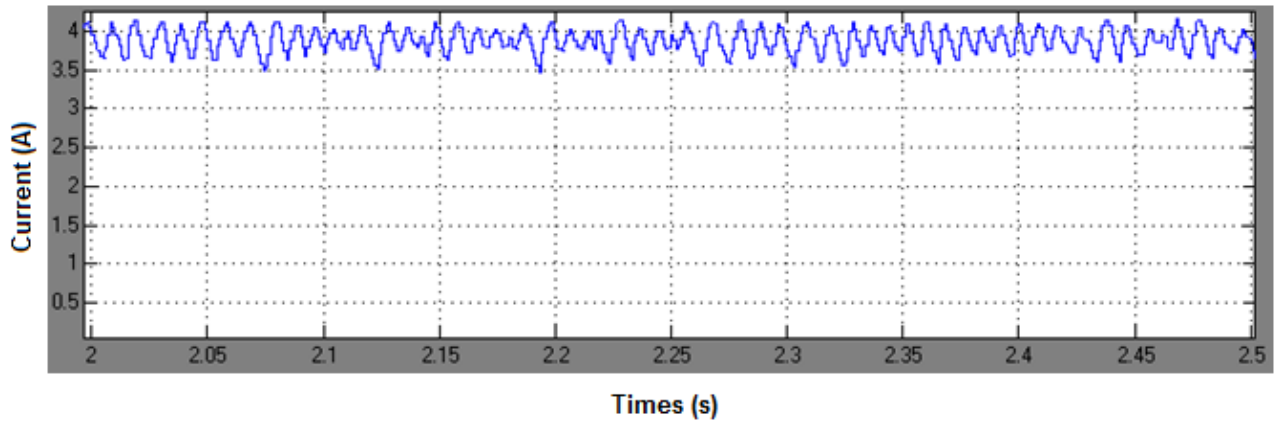

Fig. 5.6: Ipv acquisition

The fig.5.7 that presents the maximum power point tracking shows that the power delivered from the module is around 160 W. in the absence of a proper equipment to measure the sunlight irradiance we can use the data from the table 5.3 to estimate its value.

$$I_r \cong \frac{P}{\eta * A} \tag{45}$$

$$I_r \cong \frac{160\ W}{0.167 * 1.28\ m^2} \tag{46}$$

$Ir \cong 748.5\ W/m^2$

So, it means that the normal irradiance over the module during the experimental tests was approximately 750 W/m^2, assuming that the temperature was not so different of 25ºC.

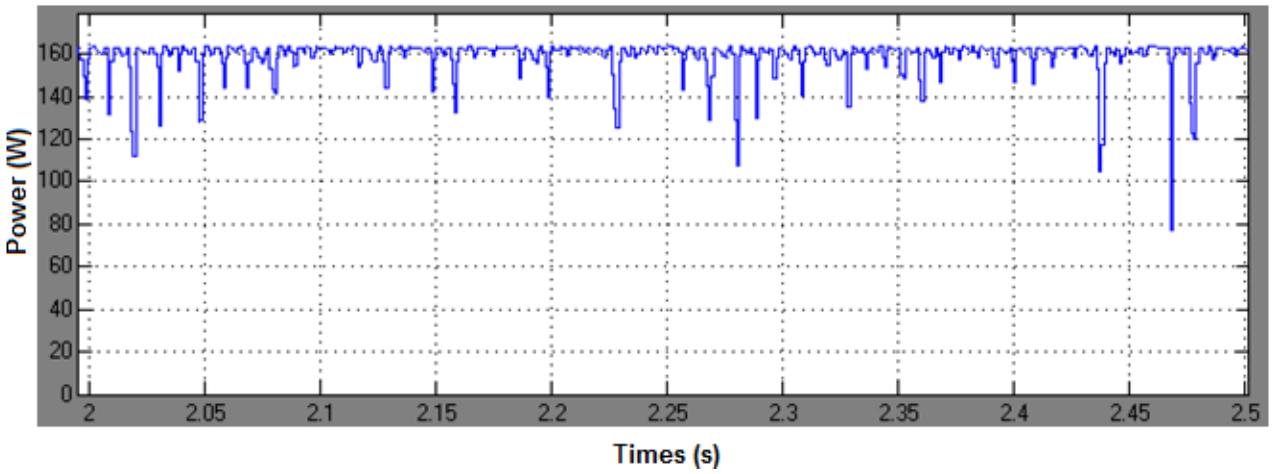

Fig. 5.7: Maximum power point tracking

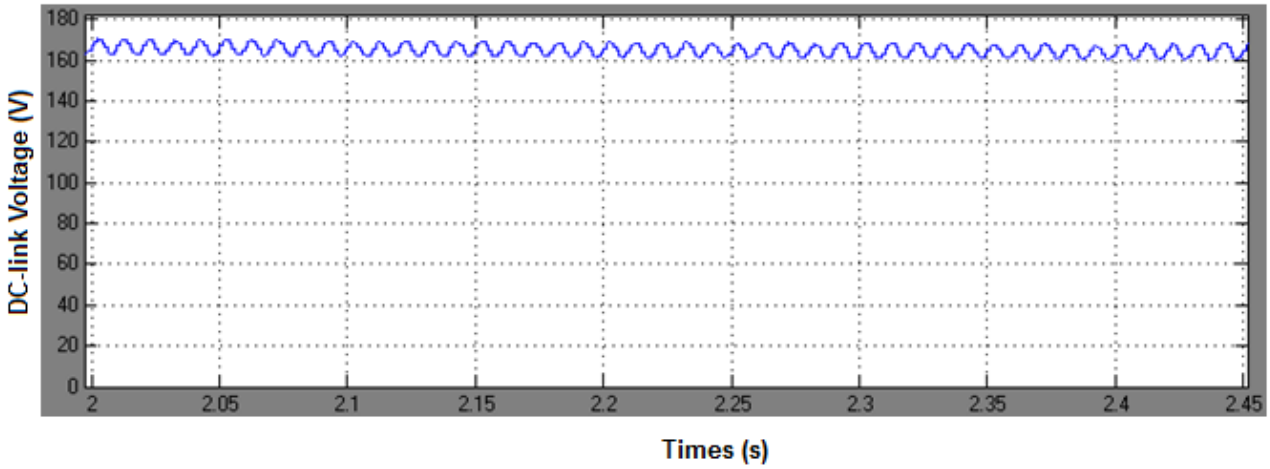

Fig. 5.8: DC-link voltage measurement

The measured dc-link voltage, fig. 5.8, is compared to the reference voltage and then the error signal passes through the PI controller to acquire the proper compensation value for output current reference (Ciobotaru et al). It is important that the DC-link voltage to be stable to have an output current with good quality. The amplitude of the voltage varies with the amount of energy delivered from the module.

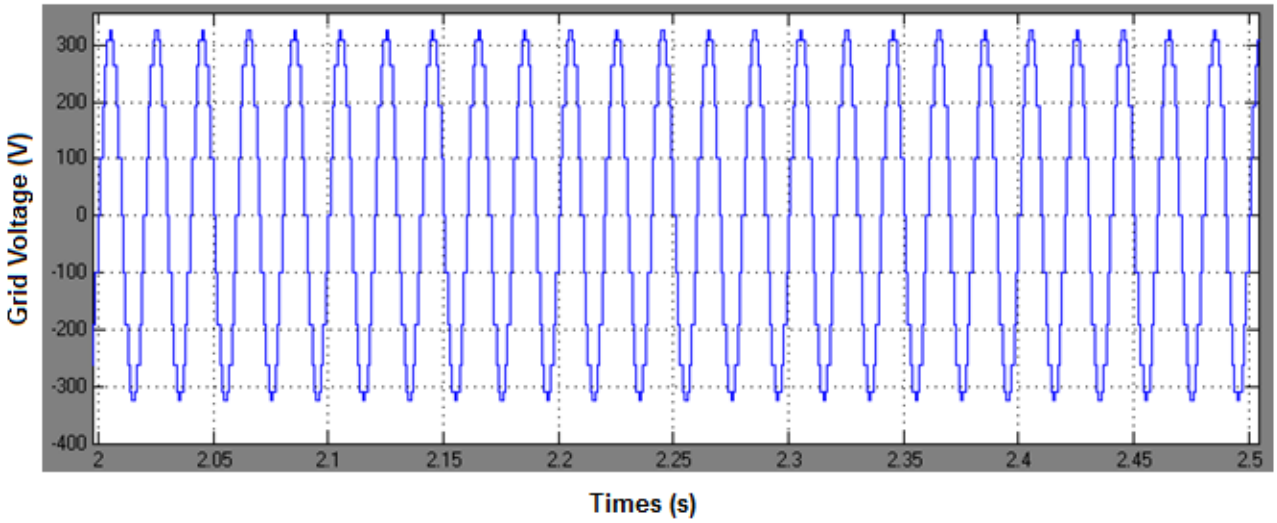

Fig. 5.9: Grid voltage

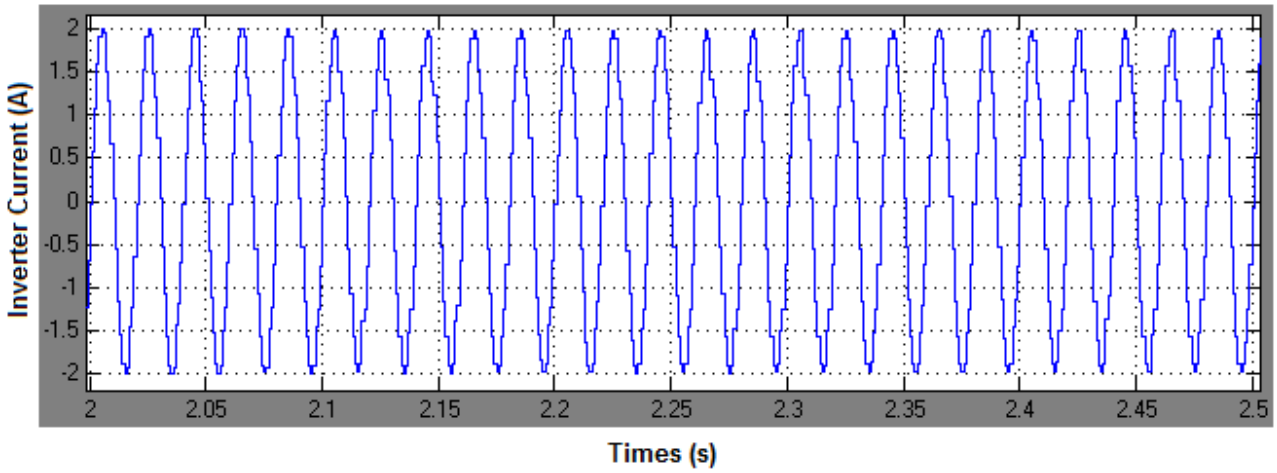

Fig. 5.10: Output current of the inverter

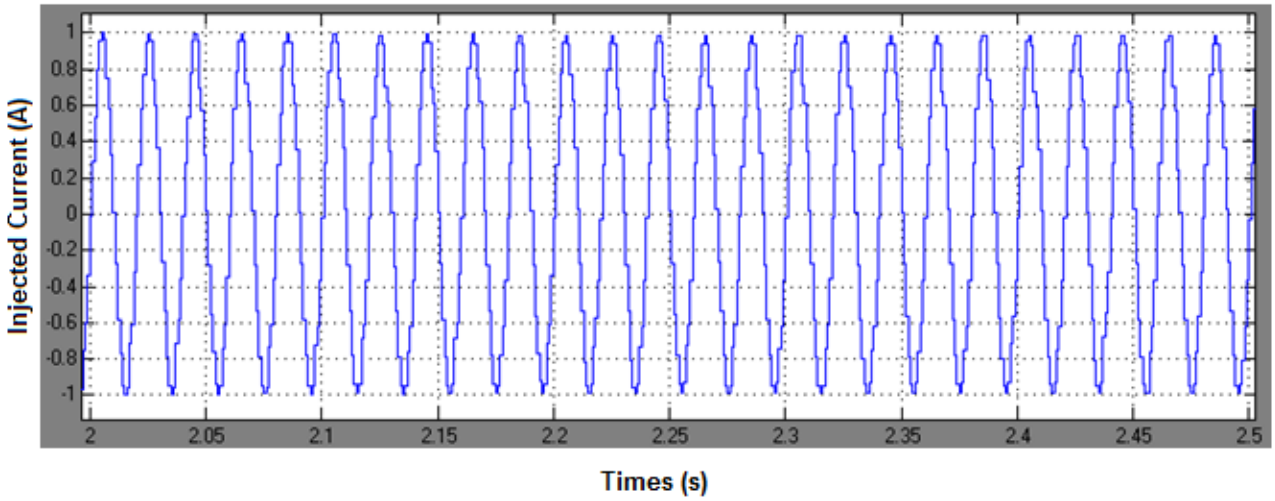

Fig. 5.11: Current injected to the grid network

The Fig. 5.9 represents the grid voltage. The knowledge of its value is necessary for the PLL operation in the sliding mode of current.

The fig. 5.10 and fig. 5.11 represents the current in the primary and secondary of the transformer respectively. The current in the primary of the transformer is the one that results from the sliding mode of the inverter its amplitude depends directly of the power delivered from the module and its frequency and phase are set by the PLL according to the grid values. The current in the secondary of the transformer is the one that is injected to the grid network. It has half amplitude of the primary.

The principal inconvenient of the power electronic devices when connected to the grid is the content of harmonic pollution that is injected into the network system. The harmonics deteriorate the quality of the energy and produce lot of losses. So, every equipment of this kind must obey the norm IEC 61000-2-2 that regulate the total harmonic distortion of the voltage (47) and current (48) and power factor (49) of the customer equipment.

$$THD_v = \sqrt{\left(\frac{V_{rms}}{V_1}\right)^2 - 1} \tag{47}$$

$$THD_i = \sqrt{\left(\frac{I_{rms}}{I_1}\right)^2 - 1} \tag{48}$$

$$PF = \frac{P}{S} \tag{49}$$

$$S = \sqrt{P^2 + Q^2 + D^2} \tag{50}$$

Where, *S* represents the Total Power, *P* the Active Power, *Q* the Reactive Power and *D* Distortion Power.

In the grid tied PV system the PLL control synchronizes the phase of current with the grid voltage, therefore, the reactive power is null. The fig. 5.12 represents the active power and the power relative to the harmonic content injected to the grid.

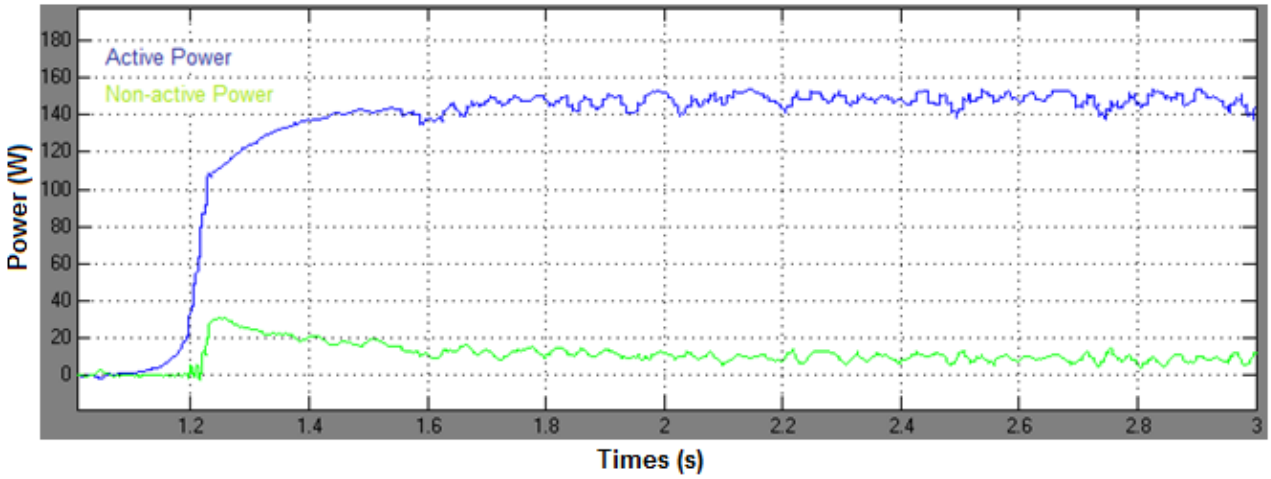

Fig. 5.12: Active and Distortion Power injected to the grid

The efficiency is one of the most important parameter that features the power electronics devices. An inverter is built mainly to convert DC power to AC power so its efficiency is defined as:

$$\eta = \frac{P}{P_{DC}} \tag{51}$$

Table 5.4 summarizes the inverter parameters under these test conditions.

Table 5.4: Inverter features at test conditions

$V_{PV(average)}$	42.1 V
$I_{PV(average)}$	3.8 A
$P_{DC(average)}$	160.0 W
DC-link voltage (V_{DC})	162.4 V
$I_{g(rms)}$	0.627 A
Active Power (P)	146.9 W
Distortion Power (D)	9.1 VA
THD of I_g	9.8 %
Power Factor (PF)	0.998
Efficiency (η)	91.8 %

Chapter 6

Conclusions and future work

6.1 Conclusions

This present work studies the many topologies of the inverters existent in the literature, industry or commercialized, and chose an optimal solution for the module scale application to be implemented and tested in the field. After study the many topologies to see the pros and cons, and see the simulation results in MatLab Simulink the choice came to the two-stage single-phase inverter with the LF transformer. This topology is composed of a DC-DC converter proceeded by a DC-AC converter and o low-frequency transformer.

The DC-DC converter is a boost that elevates the voltage provided from the PV module while it's doing the MPPT to find the optimal operating point of the module. The boost is composed by the the inductor, switching transistor, ultra-fast diode and capacitor (fig. 4.6), the measuring sensors and the auxiliary control and feeding circuits.

The DC-AC converter is a full-bridge inverter that operates in the sliding mode of current. The transistors used in the full-bridge and the one used in the boost converter are both IGBTs from a single module (fig. 5.4), that is integrated within its respective driver circuits. The module is composed by a three arms full-bridge IGBTs.

The control of both boost converter and the full-bridge inverter is done by the Arduino Uno controller board that performs the MPPT algorithm and the sliding mode of current control. The script code is written in C language in the Arduino environment and is provided in the Annex I.

The tests were performed in the laboratory using an electric font and a PV module. Using the PV module turned to the sunlight the average DC power measured in the input of the device was approximately 160 W which according to the equation (45) corresponds to an irradiation of 750 W/m^2. The PV input signals have some undesirable ripple which is generated by the constant

change of the duty cycle provided by the “perturb and observe” MPPT algorithm. This algorithm should be improved so the duty cycle only changes when a relevant change of conditions is observed.

According with the test conditions the inverter turns out to be very efficient presenting an efficiency of 91.8%. This efficiency is obtained following the equation (51). For a more detailed desdcription of the efficiency it was necessary experimental trials with various levels of irradiation using a solar simulator. So, we would analyze the behavior of the inverter under many input power and trace the curve of efficiency.

The harmonic content is a very important parameter when it comes to a device connected to the grid. Therefore, I have done an analysis of the quality of power injected to the grid, using the parameters *THDi* of the current and the *PF*. According with the norm IEC 61000-2-2 a *THDi* between 10 and 50% shows a significant harmonic pollution, and a value under 10% is classified as normal. Using the equation (48) I obtained a *THDi* of 9.8% which reveals that the device fulfills the norm. A *PF* of 0.998 is also a good indicator.

6.2 Future work

The mainline objective of this work was to develop a reliable and cost-effective prototype of PV inverter. Several studies were performed on the prototype, and several more should be done as a continuation of this work.an economical study of the device that was not possible to carry out in this present work is still required.

The concern about reducing the cost and size/weight of the device encourages the study of a transformerless topology solution that could be the line of continuation of this work. The replacement of the voltage transducers for the simple voltage dividers in the V_{PV} and V_{DC} measurement would reduce a lot the device cost, once these transducers are quite expensive. The use of Arduino controller itself, despite of its great versatility and facility of use could not be economically the best choice for a commercial inverter. So, a cheaper microcontroller must be considered.

It would be desirable to develop a prototype in a PCB where all the components were strategically placed so that the control circuit would be closer to the sensors and IGBT drivers which would reduce the noise in the control signal

References

Alsema,E. and Nieuwlaar,E. *Environmental aspects of PV power systems.* 97072. IEA PVPS Task 1 Workshop, Utrecht, the Netherlands, 1997.

Blaabjerg, F. *Power Electronic in the Renewable Energy Systems.* Aalborg University - Institute of Energy Technology, DK, 2006.

Carbone, R. *Energy Storage in Grid-Connected Photovoltaic Systems*. *University "Mediterranea" of Reggio Calabria*- Italy, 2010.

Carbone, R. *Grid-Connected Photovoltaic Systems with Energy Storage*. *Proceeding of IEEE International Conference on CLEAN ELECTRICAL POWER, Renewable, Energy Resources Impact "ICCEP 2009"*. Capri – Italy, June 9-11, 2009.

Chaudhari, V. *Automatic Peak Power Tracker For Solar Pv Modules Using Dspacer Software*. Maulana Azad National Institute Of Technology, Deemed University, India, 2005.

Ciobotaru, M; Teodorescu, R; Blaabjerg, F. *A New Single-Phase PLL Structure on Second Order Generalized Integrator*. Aalborg University – Institute of Energy Tecnology. Denmark, 2006.

Chayavanich, T; Limsakul, C; Chayavanich, N; Chenvidhya, D; Jivacate, C; Kirtikara K. *Evaluation Of Power Quality Of Pv-Grid Connected System With Battery Storage Under Low Radiation*. School Of Energy, Environment And Materials, 2. Electrical Engineering Department, 3.Ces Solar Cell Testing Center (Cssc) King Mongkut's University Of Technology Thonburi (Kmutt), Bangkok, Thailand

Chee Lim, N; Ole-Morten M; Sætre T; Norum, L. *Energy Management For Grid-Connected Pv System With Storage Battery.* University Of Agder, Faculty Of Engineering And Science, Jon Lilletunsvei 9, 4879 Grimstad, Norway Norwegian University Of Science And Technology, Department Of Electric Power Engineering, 7491 Trondheim, Norway

Dodge, J. & Hess, J. *Advanced Power Technology,* Dresden, Germany. 2002

Duffy, S. And Cathcart, T. The Photovoltaic Energy System For The MSU Sustainable House. Mississippi State University, USA, 2008

Frisch, M. & Ernö, T. *Innovative Topologies for High Efficient Solar Applications*, Vincotech GmbH, Biberger Str. 93, 82008 Unterhaching (Germany) and Vincotech Kft., Kossuth Lajos u. 59, H-2060 Bicske (Hungary),Nov. 2008

Geibel, D. *Power Quality Improvement Of Electrical Sub-Networks With Multifunctional Pv-Inverters For Industrial Customers.* Institut Fuer Solare Energieversorgungstechnik E. V. (Iset), Koenigstor 59, D-34119 Kassel, Germany, 2008.

Gosbell, V; Perera, S; Smith, V. *Harmonic Distortion On The Electric Supply System*. Power Quality Center, University Of Wollongong, Australia, 2000

Lega, A. *Multilevel Converters:Dual Two-Level Inverter Scheme*. Department Of Electrical Engineering, University Of Bologna, Italy, 2007

Liserre, M; Blaabjerg,F; Teodorescu, R; Aalborg, Z. *Power Converters and Control of Renewable Energy Systems*. The 6-th International Conference on Power Electronics, 2004.

Mohanty, P. and Sahoo, S. *Analysis Of Two Level And Three Level Inverters*. Department of Electrical Engineering, National Institute of Technology, Rourkela, India, 2010

Mohapatra, M. and Babu, B. *Fixed and Sinusoidal-Band Hysteresis Current Controller for PWM Voltage Source Inverter with LC Filter*. Department of Electrical Engineering, National Institute of Technology, Rourkela, India, 2010.

Maurice, B. and Wuidart, L. *Drive Circuits For Power MOSFETs And IGBTs*

Ross,M. and Royer,J. *Photovoltaics in cold climates*. James & James Ltd, Malta, 1999.

Sørensen,B. *Renewable energy: Its physics, engineering, use, environmental impacts, economy and planning aspects.* Academic Press, Great Britain, 2000.

Ueda, Y; Kurokawa, K; Itou, T; Kitamura, K; Akanuma, K; Yokota, M; Sugihara, H; Morimoto, A. *Performance analyses of battery integrated grid-connected residential PV systems.n Proceeding of 21st European Photovoltaic Solar Energy Conference*, 4-8 September 2006,

WADE. *Guide to decentralized energy technologies.* World Alliance for Decentralized Energy, Edinburgh, Great Britain, 2003.

Watt,M. *Added values of photovoltaic power systems.* IEA-PVPS, Australia, 2001.

EPIA and Greenpeace. *Solar generation - Solar electricity for over 1 billion people and 2 million jobs by 2020.* European Photovoltaic Industry Association & Greenpeace International, 2004.

EPIA. EPIA Roadmap. *European Photovoltaic Industry Association*. Brussels, Belgium, 2004.

United States Photovoltaics Industry. *Solar electric power - the U.S. photovoltaic industry roadmap.* National Renewable Energy Laboratory, 2003.

http://www.volker-quaschning.de

Annex I

Script code for Arduino board control

```
/*
 * Two Stage Single Phase Inverter control
 *
 * JN. Barbosa - MERCEUS - DEE - FCT-UNL
 */

 float Vpv0 = 0.00; // inicials conditions
 float Ipv0 = 0.00;
 float P0 = 0.00;
 float Vpv1 = 0.00;
 float Ipv1 = 0.00;
 float P1 = 0.00;
 float D = 0.50; // duty-cycle
 float dD = 0.01; // perturbation

 void setup()
 {
   Serial.begin(9600);

   TCCR2B = TCCR2B & 0b11111000 | 0b11; // set the output frequency to 3906.25hz

   pinMode(3, OUTPUT);  // sets the pin as output
   pinMode(9, OUTPUT);  // sets the pin as output
   pinMode(10, OUTPUT);
 }

 void loop()
 {

   Vpv0 = analogRead(0); // read the pv voltage
   Vpv0 = map(Vpv0,0,1023,0,60.6); // conversion to real voltage value

   Ipv0 = analogRead(2); // read the pv current
   Ipv0 = map(Ipv0,0,1023,0,15.0);


   P0 = Vpv0*Ipv0;              // calculate instant power

  delayMicroseconds(100);

  Vpv1 = analogRead(0); // read the pv voltage
```

```
 Vpv1 = map(Vpv1,0,1023,0,60.6);

 Ipv1 = analogRead(2);
 Ipv1 = map(Ipv1,0,1023,0,15.0);

 P1 = Vpv1*Ipv1;

 int dV = Vpv1-Vpv0;
 int dP = P1-P0;

if (dP > 0){
  if (dV > 0){
    D = D+dD;
  }else{
    D = D-dD;
  }
}else {
  if (dV > 0){
    D = D-dD;
  }else{
    D = D+dD;
  }
}

analogWrite(3,D*255);

float Vdc = 0;
 float vg = 0;
 float Ia = 0;
 float Ig = 0;
 const float pi = 3.1415;

 vg = analogRead(3)*2;          // read grid voltage
 vg = map(vg,0,1023,0,240);

 Vdc = analogRead(5);         // read dc-link voltage
 Vdc = map(Vdc,0,1023,0,230);

 Ia = analogRead(4)*300;          // read output current
 Ia = map(Ia,0,1023,0,2);
 Ig =Ia/2;

  /* PLL structure ***
  */
  {
  float k = 0.8;
  float Ts = 1*pow(10,-4);
  float z = 1*pow(10,-4);
```

```
float omega,theta;
float s = (Ts/2*(3*pow(z,-1)-pow(z,-2))/(1-pow(z,-1)));

float v = k*omega*s/(pow(s,2)+ k*omega*s + pow(omega,2))*vg;
float qv = (k*pow(omega,2))/(pow(s,2) + k*omega*s + pow(omega,2))*vg;

float vd = v*cos(theta) + qv*sin(theta);
float vq = qv*cos(theta) - v*sin(theta);

float vqref = 0;
float erro_vq = vqref - vq;
float Kp,Ti;
float PIout = erro_vq*(Kp*(1+1/(Ti*s)));

float omegaff =50/(2*pi);
omega = omegaff + PIout;

theta = omega*1/s;

float Vmag = sqrt(pow(v,2)+pow(qv,2));


/* PI for Vdc control*/

float KP = 1.0;
float KI = 2.0;
float err_PI = Vmag/2 - Vdc;
float PI_out = err_PI*(KP + KI*Ts*1/(z-1));

if (PI_out > 1.2) {PI_out = 1.2;}    // saturation
else if (PI_out < 0) {PI_out = 0;}

/* build reference current Iref */

float Imag = 0.8*(Ipv1*Vpv1)/(Vmag/2) + PI_out;
float sinref = sin(omega*Ts + theta);
float Iref = Imag*sinref;

/* Bang-bang current control   */

float lb = 0.05;
float ihi = Iref + lb;
float ilow = Iref - lb;
float sw1;
float sw2;
float sw3;
boolean S1S4;
boolean S2S3;
```

```
if ((Ia-ihi)>0) {
sw1=-Vdc;}
else {sw1=0;
}

if (-(Ia-ilow)>0) {
sw2=Vdc;}
else {sw2=0;
}

if (abs(sw1+sw2)>0) {
 sw3=sw1+sw2;}
else {
 delayMicroseconds(10);
 sw3=sw3;
}

if ( sw3 > 0) {
  S1S4 = HIGH;
  S2S3 = LOW;
} else {
  S2S3 = HIGH;
  S1S4 = LOW;

  digitalWrite(9,S1S4);
  digitalWrite(10,S2S3);
}}
Serial.println(Vpv1);
Serial.println(Ipv1);
Serial.println(P1);
Serial.println(Ig);
}
```